

**Synthesis of dispersible and aggregatable
nanoparticle by controlling of modification
on silica surface**

シリカ表面の改質制御による分散性・凝集性粒子の合成

June, 2017

Aki Kawamura

Synthesis of dispersible and aggregatable
nanoparticle by controlling of modification
on silica surface

A Doctoral Dissertation by

Aki Kawamura

June, 2017

Graduate School of Engineering,
Department of Frontier Materials,
Nagoya Institute of Technology

Advanced Ceramics Research Center
Materials Processing

Supervisor: Prof. Masayoshi Fuji

Contents

Chapter 1: Introduction	1
Outline of study.....	1
1-1 Introduction	2
1-2 Fumed silica	3
1-3 Surface structure of fumed silica.....	6
1-4 Surface modification	8
1-5 Surface modification mechanism and modifiers.....	10
1-6 Surface modification methods	12
1-7 Characterization of modified silica surface	15
1-8. Objectives	18
References	19
Chapter 2: Effect of solvent polarity and adsorbed water on reaction between hexyltriethoxysilane and fumed silica	27
2-1. Introduction.....	27
2-2. Experimental	29
2-2-1. Materials	29
2-2-2. Surface modification.....	30
2-2-3. Characterizations	30
2-3. Results and discussion	32
2-4. Conclusion	41
References	42
Chapter 3: Effect of steric hindrance on surface wettability of fine silica powder modified by <i>n</i> - or <i>t</i> -butyl alcohol	47
3-1. Introduction.....	47
3-2. Experimental	49
3-2-1 Materials	49
3-2-2 Surface modification.....	49
3-2-3 Characteristics of silica surface	49
3-2-4 Determination of the amount of water vapor adsorption by FT-IR.....	51
3-2-5 Preference dispersion test	51

3-3. Results and Discussion	52
3-3-1 Characteristics of modified fumed silica surface	52
3-3-2 Macroscopic wettability evaluated by preference dispersion test.....	59
3-3-3 Amount of water vapor adsorption on unmodified silica observed by FT-IR.....	61
3-3-4 Microscopic wettability evaluated by the amount of water vapor adsorption by FT-IR ..	64
3-4. Conclusions.....	71
References	72

Chapter 4: Surface modification of fumed silica by photo-dimerization reaction of cinnamyl alcohol and cinnamoyl chloride

4-1. Introduction.....	77
4-2. Experimental	79
4-2-1 Materials and surface modification	79
4-2-2 Characteristics of silica surface	81
4-2-3 Determination of hydrophilic/hydrophobic	81
4-2-4 Simulation	82
4-2-5 Optical irradiation and UV spectral characteristics of modified silica surface.....	82
4-3. Results and discussion	84
4-3-1 Characteristics of fumed silica	84
4-3-2 IR spectral characteristics of silica surface	84
4-3-3 Determination of modifier introduced on silica surface.....	88
4-3-4 Determination of hydrophilic/hydrophobic	91
4-3-5 Calculation of the intermolecular distance	92
4-3-6 Simulation	93
4-3-7 Optical irradiation.....	96
4-4. Conclusion	101
References	102

Chapter 5: Summary

Achievements

Acknowledgement.....

Chapter 1: Introduction

Outline of study

Chapter 1 provides fundamental information regarding silica. This includes the methods used currently to synthesize it, its surface characteristics, the methods available for modifying its surface, and their underlying mechanisms. Further, the increase in the industrial demand for nanosized materials and the problems associated with these materials are also stated.

Chapter 2 describes an investigation of the relationship between the polarity of the organic solvent used and the amount of water adsorbed on the surface of fumed silica, with the aim of modifying the silica surface. This is an effective way of realizing surface-modified fumed silica at the molecular level. The obtained results are also discussed.

Chapter 3 describes the effects of the structure and mobility of the modifier introduced onto the surfaces of the fumed silica particles owing to wettability. It is shown that the structure and mobility of the modifier control the surface modification process at the molecular level.

Chapter 4 describes the synthesis of a novel dispersible and aggregatable silica-based nanomaterial by the modification of the surfaces of fumed silica nanoparticles based on the knowledge presented in Chapters 2 and 3. It is confirmed that the modified silica is highly dispersible and aggregatable when subjected to UV irradiation.

Chapter 5 summarizes the results of the study.

1-1 Introduction

Nanoparticles 1–100 nm in size have become indispensable materials in various fields, including in materials science [1–3], medicine [4–6], and cosmetics [7–9], because their physical and chemical properties can be controlled to a greater degree than those of particles larger than 100 nm. Controlling the dispersion stability of nanoparticles in various liquid media or solid matrix materials is essential for controlling the properties of the final products [10].

Nanoparticles show a high degree of adhesion and a propensity to undergo aggregation because they exhibit Brownian movement and because their surfaces are activated [11, 12]. Thus, when using nanoparticles as a raw material, being able to control their dispersibility and aggregation becomes critical.

Nanosized particles are being used in many industrial fields. In such cases, the surface properties of the particles determine the properties of the final material. To ensure that the nanoparticles being used have the desired effect, they should be uniformly dispersed in the medium in question [13–15]. On the other hand, the material which can be shaped by irradiation of laser or ultraviolet technic [16–19] is nanosized because of the recent development proceed of three-dimensional (3D) technology [20, 21].

The dispersibility and aggregation of nanoparticles in various media, which are key factors, are determined by their surface structure and properties. For example, if the nanoparticles are to be

dispersed in water, their surfaces should be hydrophilic. In contrast, if the nanoparticles are to be dispersed in an organic solvent or resin, their surfaces should be modified to exhibit a high affinity for the organic solvent in question, meaning that their surfaces should be made hydrophobic [22, 23].

The surfaces of inorganic oxide particles are hydrophilic owing to the presence of hydroxyl groups [12, 24–28]. The surfaces are modified based on the type of organic functional groups present in the medium being used and their content. This is done by replacing the surface hydroxyl groups with other organic functional groups. Several researchers have studied surface-modification reactions between hydroxyl groups and organic functional groups [29–31]. It has been suggested that the dispersibility and aggregation of nanoparticles can be controlled by selecting the appropriate functional groups and introducing them on the surfaces of the nanoparticles. In addition, the surface modification rate determines the wettability of the surfaces of the nanoparticles, meaning that it also affects their dispersibility and aggregation as they relate to various applications.

1-2 Fumed silica

Fumed silica is used in various applications to improve the functionality of different materials.

Some of these applications are listed below [32–39];

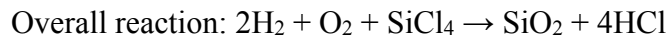
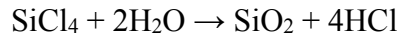
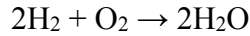
- Paints and coatings
- Catalysts
- Airbags
- Silicone sealants used in cars, sanitaryware, and electronics

- Sealing inserts (e.g., for covering the crown cork)
- Printing inks
- Creams, lotions, and gels
- Deodorants
- Paper properties
- Chemical dowels
- Unsaturated polyester resins
- Light bulbs and fluorescent tubes
- Toners for photocopying machines
- Silicone profiles
- Shoe soles
- Putty
- Dental composites
- Two-component mortars
- Marine paints
- Structural adhesives used for producing rotor blades for wind power plants
- Varying the dosability of active substances in tablets
- High-tension cables
- Adhesives (e.g., instant glue and hot-melt adhesives)

For all these applications, being able to control the dispersibility of fumed silica in the medium being used, which could be an organic solvent, polymer, or water, is essential. However, it is well known that fumed silica nanoparticles are highly hygroscopic and exhibit a high degree of agglomeration. Thus, to be able to use fumed silica in the above-listed applications, it is essential to control their dispersibility and agglomeration.

Fumed silica is manufactured by the continuous-flame hydrolysis of substances such as silicon tetrachloride (SiCl_4). In the flame, hydrogen and oxygen (from the air) react in the presence of SiCl_4 . The formation of SiO_2 occurs through the combination of an oxyhydrogen reaction, in which water is

formed, and the hydrolysis of SiCl₄ because of the formed water. The process can be expressed by the following equations [40]:



Many of the properties of fumed silica can be described using a simplified droplet model. This model assumes that the reaction gases pass through a region that results in an initial sharp increase in the temperature and a subsequent decrease the flame. At the start of the reaction (at the base of the flame), minute droplets of SiO₂ are formed (nuclides). These nuclides collide with one another stochastically and merge to form bigger and heavier droplets. These bigger droplets can then merge with others and so on the overall number of droplets keeps decreasing as the droplet size increases. This process continues till the flame is hot enough to keep the droplets in the liquid state. When the droplets enter a colder area of the flame, they solidify (at least partially). When these droplets collide, instead of fully merging and coalescing to form larger spherical droplets, they merge only partially. This results in aggregates consisting of primary particles (the partially solidified droplets).

The aggregates solidify completely in the colder parts of the flame. When these aggregates collide, they are unable to merge. Instead, they attach to each other and are held together by weak interactions.

This results in the formation of agglomerates. This droplet model of particle genesis is illustrated in

Fig. 1-1 [41].

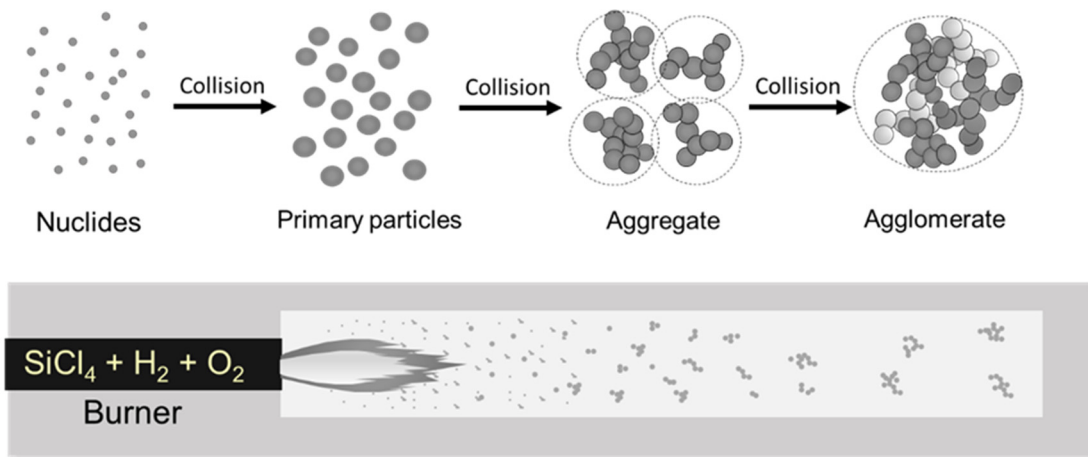


Fig. 1-1 Schematic illustrating simplified model of particle genesis in flame.

1-3 Surface structure of fumed silica

The surface of fumed silica contains two types of functional groups, namely, the silanol group and the siloxane group. These structures are shown in Fig. 1-2. The silanol groups are responsible for the hydrophilicity of the surface of fumed silica while the siloxane groups are responsible for the hydrophobicity. Agglomeration is caused by the activation of the silanol groups on the fumed silica surface [42].

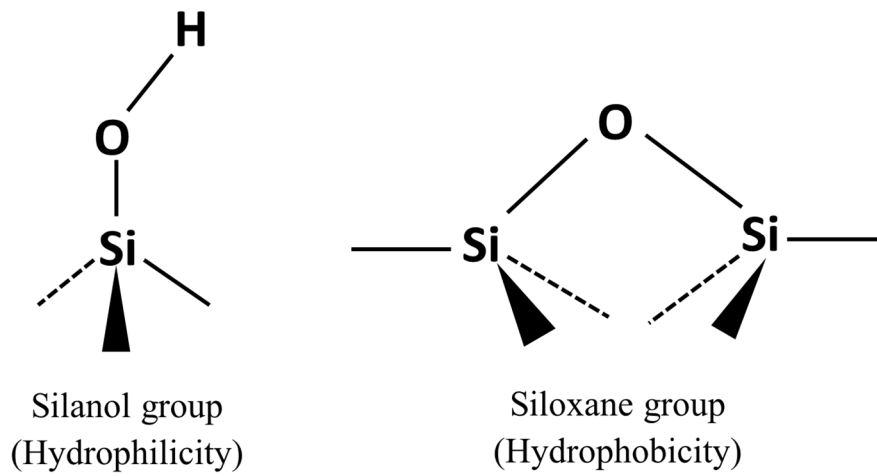


Fig. 1-2 Silanol groups (left) and siloxane groups (right).

Figure 1-3 shows the hydrogen-bond-based interaction between two fumed silica particles. The probability of a silanol group finding another silanol group to form a hydrogen bond increases with a decrease in the particle size. Therefore, the number density of the unbonded silanol groups decreases as the specific surface area increases. This, in turn, decreases the dispersibility of the fumed silica particles and the particles readily undergo aggregation by forming hydrogen bonds with each other [43].

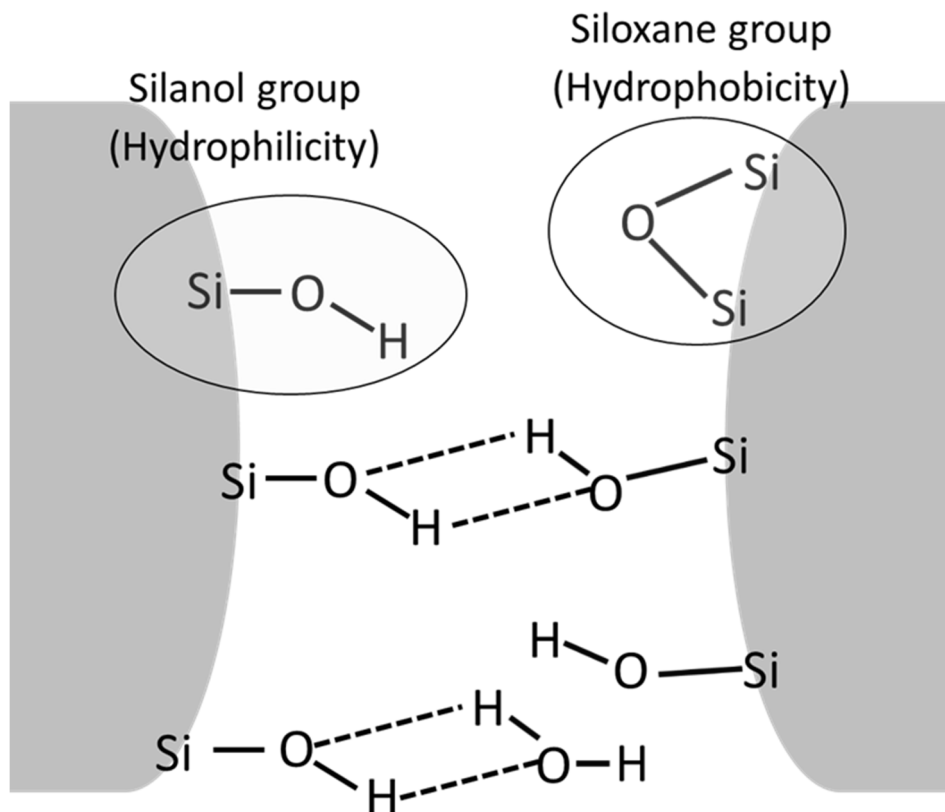


Fig. 1-3 Formation of hydrogen bonds between two fumed silica primary particles.

1-4 Surface modification

As mentioned above, fumed silica particles readily form aggregates. However, they must exhibit high dispersibility for use in various applications. Methods of preventing aggregate formation have been studied by several researchers. The main method of preventing fumed silica from undergoing aggregation is to modify the silica surface using organic functional groups.

A schematic of a typical silica surface modification process is shown in Fig. 1-4 and 1-5 [44].

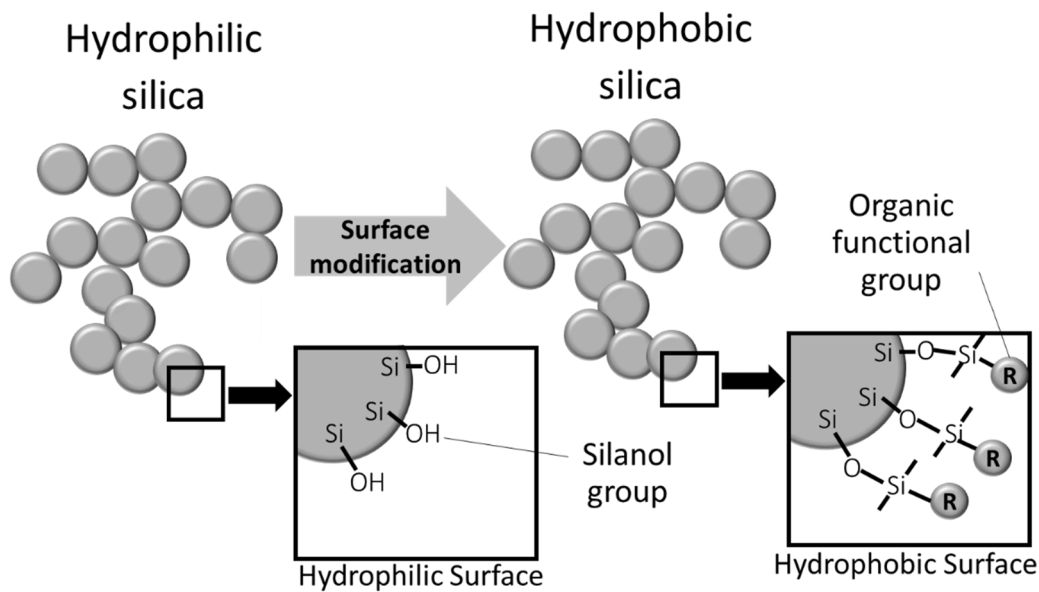


Fig. 1-4 Schematic of surface treatment for transforming hydrophilic fumed silica into hydrophobic fumed silica.

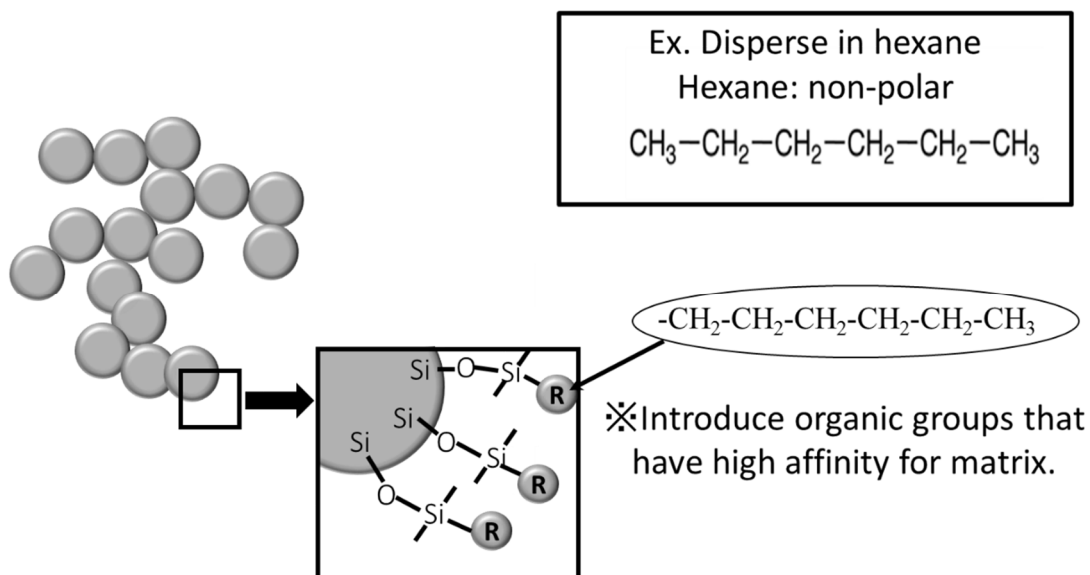


Fig. 1-5 Schematic of surface treatment of hydrophobic fumed silica to allow for dispersion in hexane.

1-5 Surface modification mechanism and modifiers

During the liquid-phase reaction, the surface modification process occurs as follows [45]:

- The modifier undergoes hydrolysis with water, resulting in the formation of the SiOH group.
- Hydrogen bonds form between the SiOH groups of the hydrolyzed modifier and the SiOH groups on the silica surface.
- The dehydration of the bonds formed between the SiOH groups results in the formation of covalent bonds.

The reaction mechanism for surface modification is shown in Fig. 1-6 [46–48]. Functional groups appropriate for the dispersion medium being used should be chosen, as mentioned in Fig. 1-5. A few commonly used modifiers are listed in Table 1-1.

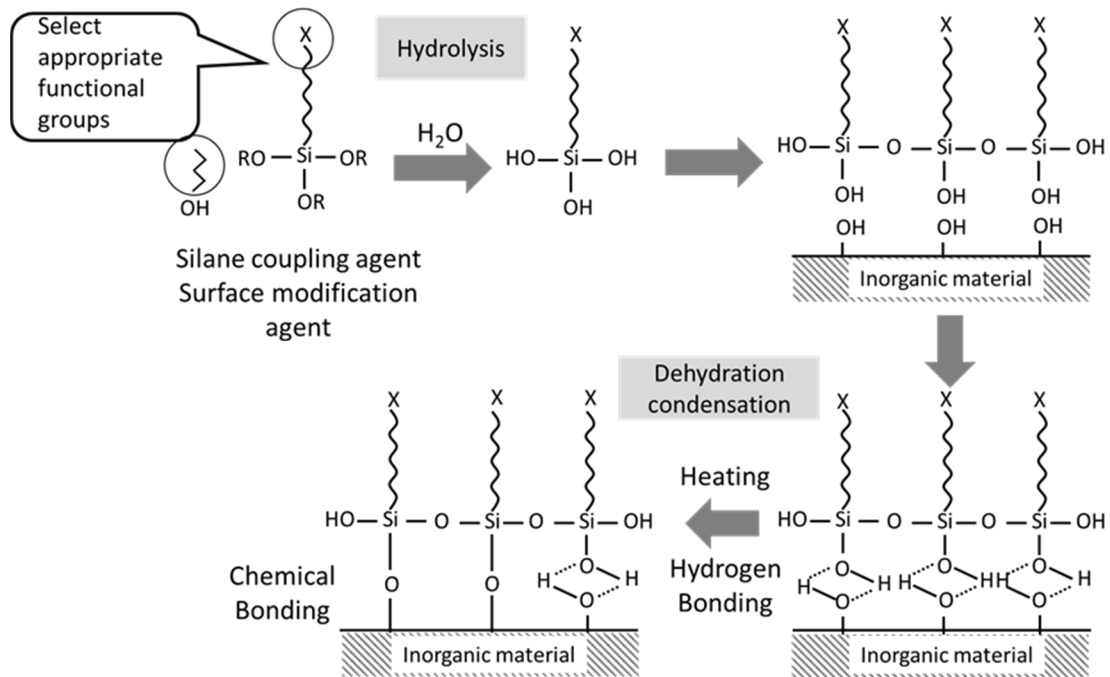
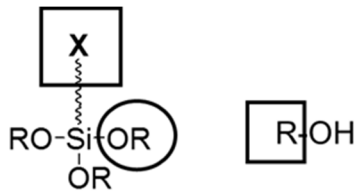


Fig. 1-6 Schematic of mechanism underlying modification of silica surface.

Table 1-1. Examples of modifiers used commonly for surface modification [47, 49]



Alcohol	X	e.g.	
Alkyl group	$-(\text{CH}_2)_n-\text{CH}_3$	CH ₃ OH, CH ₃ (CH ₂) ₂ CH ₂ OH	
Coupling agent	X	Y	e.g.
Vinyl group	$-\text{C}(\text{R})=\text{CH}_2$	Cl, -OCH ₃ , -OC ₂ H ₅	(OCH ₃) ₃ Si-(CH ₂) ₃ -CH=CH ₂
Styryl group		Cl, -OCH ₃ , -OC ₂ H ₅	
Acrylic group	$-\text{O}(\text{C}=\text{O})\text{C}(\text{R})=\text{CH}_2$	Cl, -OCH ₃ , -OC ₂ H ₅	(OCH ₃) ₃ Si-(CH ₂) ₃ -O(C=O)CH=CH ₂
Amino, Imino group	-NH₂	Cl, -OCH ₃ , -OC ₂ H ₅	(OCH ₃) ₃ Si-(CH ₂) ₃ -NH ₂
	$-\text{NH}-\text{R}-\text{NH}_2$	Cl, -OCH ₃ , -OC ₂ H ₅	(OCH ₃) ₃ Si-(CH ₂) ₃ -NH-C ₂ H ₄ -NH ₂
	$-\text{NH}-\text{R}$	Cl, -OCH ₃ , -OC ₂ H ₅	
Isocyanate group	-N=C=O	Cl, -OCH ₃ , -OC ₂ H ₅	(OCH ₃) ₃ Si-(CH ₂) ₃ -N=C=O
Epoxy group		Cl, -OCH ₃ , -OC ₂ H ₅	
Disilazane,	X	e.g.	
Alkyl group	$-(\text{CH}_2)_n-\text{CH}_3$	(H ₃ C) ₃ -Si-N=N-Si-(CH ₃) ₃	
Vinyl group	$-\text{CR}=\text{CH}_2$	(CH ₂ =CH) ₃ -Si-N=N-Si-(CH ₂ =CH) ₃	

✘ Structure of R of figure is not limited

Next, we discuss silane coupling agents, which are among the most commonly used surface modifiers.

Silane coupling agents contain two types of reactive functional groups, which exhibit different reactivities. The molecular structure of silane coupling agents is shown in Fig. 1-7. The agents react with water (undergo hydrolysis) to form silanol groups, while oligomers are formed through particle condensation. The silanol oligomers then form hydrogen bonds with the surface of the inorganic material. Finally, the inorganic material is subjected to a drying process, which leads to the formation of robust chemical bonds through a dehydration condensation reaction.

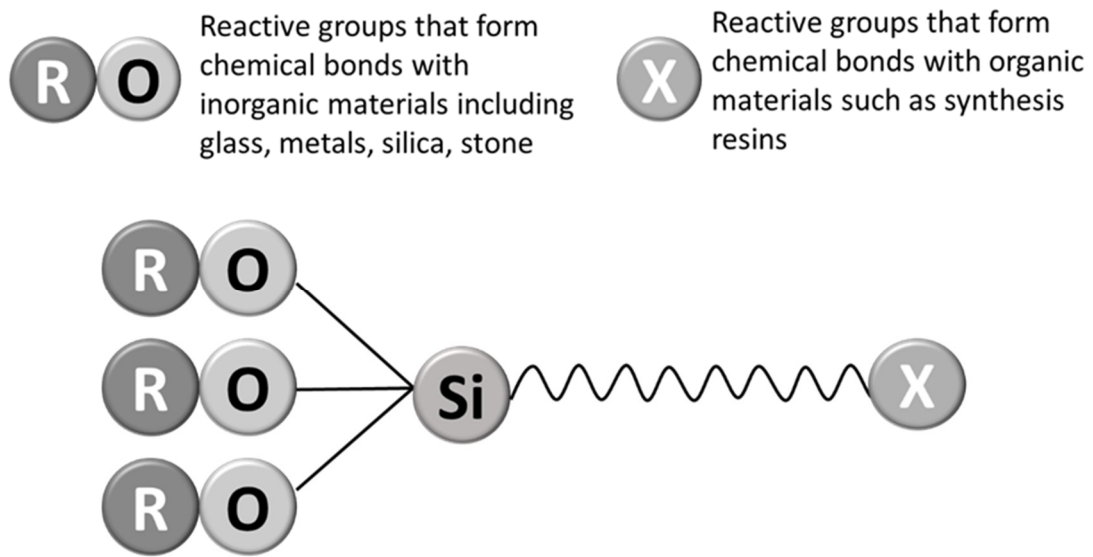


Fig. 1-7 Molecular structure of silane coupling agents [48, 49].

1-6 Surface modification methods

In this paragraph, we explain the various chemical methods used for surface modification. These methods can broadly be categorized as wet and dry methods. The methods that involve the use of an organic solvent as the dispersion media are called non-aqueous wet methods, while those that use water as the medium are called aqueous methods. Further, mixtures of water and an organic solvent can also be used as the dispersion medium. On the other hand, in the case of dry methods, such as the gas-phase method, the modifier is made to react in the presence of a decompression or carrier gas. Further, these methods involve mechanical mixing. Methods requiring mechanical mixing are primarily used in the industry.

With respect to the wet methods, the surfaces of the nanoparticles can be modified uniformly.

This is an advantage of these methods. The most common wet method is the reflux method. The reflux method can be performed using a simple setup, which is shown in Fig. 1-8. The organic solvents that are used with the reflux method are listed in Table 1-2 [50].

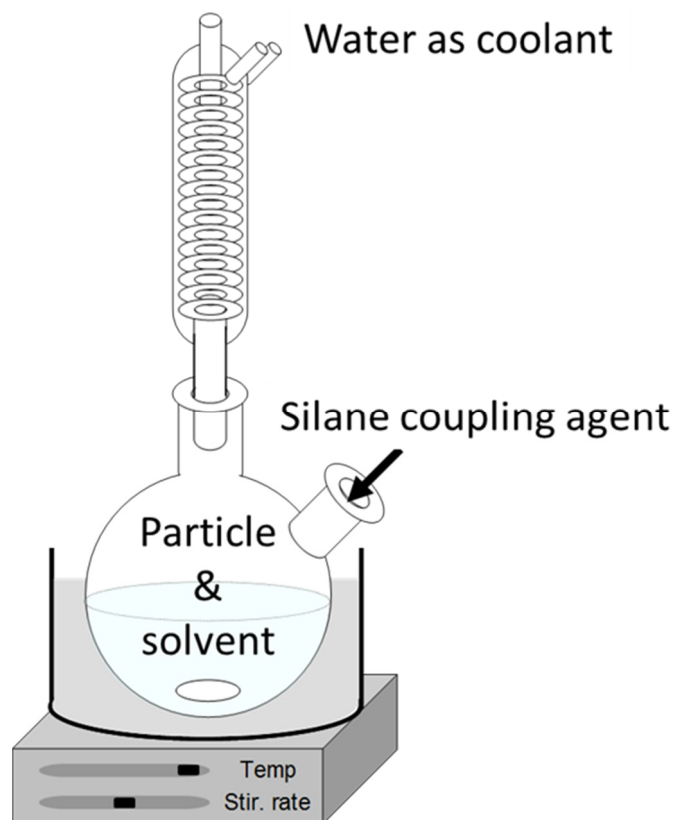


Fig. 1-8 Setup used for reflux method.

Table 1-2. Organic solvents used with reflux method [50, 51]

Solvent	B.P. [°C]	Relative permittivity [-]
Hexane	68.75	1.8
1,4-Dioxane	101.5	-
Xylene	138.35~144.15	2.4
THF	64.85	7.5
Toluene	110.65	2.4
Benzen	80.05	2.3
Acetone	56.05	20.7
MEK	79.55	15.5
DMSO	189	45

Another wet method is the autoclave method, in which the particles and the modifier are made to react in the solvent at the critical temperature of the solvent. A schematic of the autoclave method is shown in Fig. 1-9 [50, 52, 53].

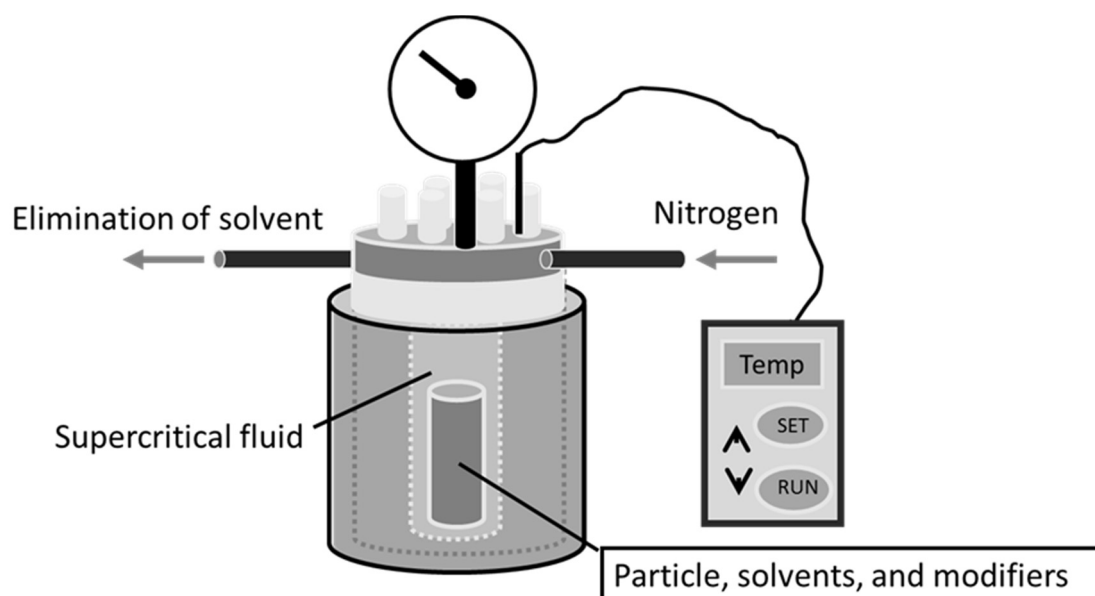


Fig. 1-9 Schematic of autoclave method.

The particle modification rate of the autoclave method is high because the amount of modifier

that can be made to react with the particles is greater than that in the case of the reflux method.

The amount of modifier to be added is determined based on the assumption that the modifier forms a monomolecular layer on the particle surface. The following equation can be used to determine the amount of modifier needed [50];

$$w_s = \frac{S_p \times w_p \times M_s \times H_p}{A} \times 10^{18} \quad (1)$$

where w_s is the amount of modifier to be added (g), S_p is the BET specific surface area of the particles in question, as measured from their nitrogen adsorption isotherm ($\text{m}^2 \cdot \text{g}^{-1}$), w_p is the weight of the modified particles (g), M_s is the molecular weight of the modifier ($\text{g} \cdot \text{mol}^{-1}$), H_p is the number density of the hydroxyl groups on the surfaces of the particles (nm^{-2}), and A is Avogadro's number. The value obtained using this equation is taken as the reference amount, and the actual amount of modifier is 1–10 times this value, as determined based on experience.

1-7 Characterization of modified silica surface

Knowing the structural and other properties of the particle surfaces is necessary for modifying them. The functional groups present on the surfaces, which include the hydroxyl groups and the organic functional groups introduced, and the adsorption properties of the particles can be investigated using various methods. With respect to the characterization of the modified particle surfaces, the amount of modifier used should be known. In general, the amount of modifier used can be determined

based on the decrease in weight owing to thermal decomposition during thermogravimetric and differential thermal analysis (TG-DTA) [50, 54–56]. The TG-DTA measurements are performed in air or oxygen and allow for the qualitative evaluation of the surface functional groups.

On the other hand, the surface wettability can be evaluated using the dispersion test, whose underlying mechanism is the opposite of weight loss. If the hydroxyl groups remain on the particle surfaces after the surfaces have been modified, they will act as adsorption sites for water molecules. Thus, this method is a simple one. The amount of water adsorbed, which is indicative of the surface wettability of the particles, can be determined using Fourier Transform infrared spectroscopy (FT-IR) [54, 57]. Observation methods can be classified as being microscopic or macroscopic, based on their scale of observation. Example of macroscopic and microscopic observation methods are shown in Fig. 1-10 and Fig. 1-11, respectively.

Thus, various methods are available for characterizing the modified particles. To characterize the surface properties of the particles, different methods should be used, and the obtained results should be analyzed in combination. Obtaining both macroscopic results and microscopic results is essential for modifying the particle surfaces such that the particles are suitable for the application in mind.

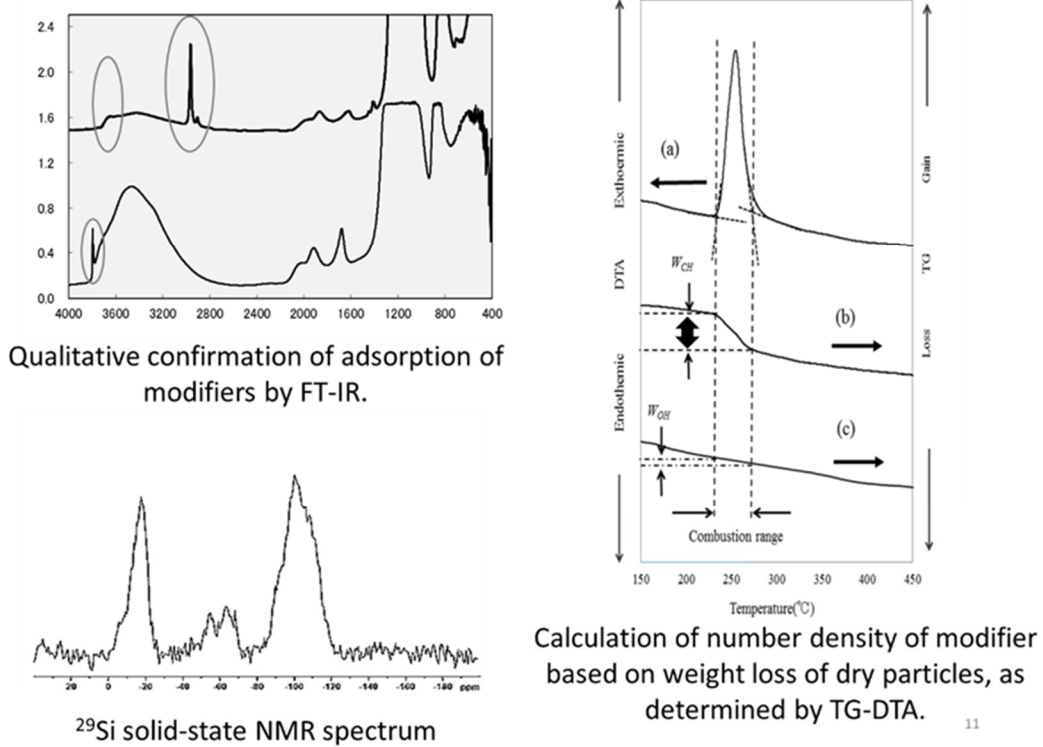


Fig. 1-10 Microscopic methods for evaluating modified particle surfaces [50, 58–61]

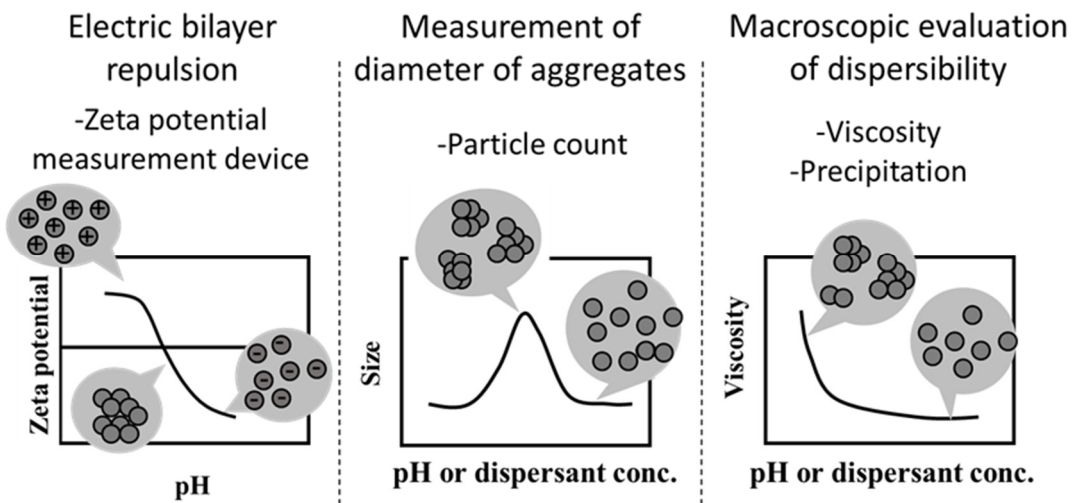


Fig. 1-11 Macroscopic methods for evaluating modified particle surfaces [61–64]

1-8. Objectives

In the past few years, the demand for functionalized particulate materials has increased significantly. Further, there has been considerable development in the synthesis of such particulates at the nanoscale. The specific surface areas of particles increase with a decrease in their size. As a result, nanoparticles exhibit a high degree of aggregation. Thus, controlling the aggregation and dispersion of nanoparticles in various media has become a critical issue, as nanoparticle aggregation can result in significant performance degradation. Thus, various methods are being explored for controlling the aggregation behavior of silica nanoparticles. The surface modification of fumed silica particles is a widely used method for improving their dispersibility in various media and has been investigated by many researchers. However, few researchers have investigated modified surfaces at the molecular level. Molecular-level observations of the fumed silica surface should yield useful information for designing functional nanosized materials.

In this study, silica nanoparticles that are dispersible and aggregable in various media were synthesized with the aim of exploring methods of controlling their dispersibility/aggregation. In addition, the surfaces of the modified silica are investigated to know their functional characteristics at a molecular level. The feasibility for using these as novel nano functional materials is explored.

References

- [1] P. Mukherjee, C. R. Patra, A. Ghosh, R. Kumar, M. Sastry, Characterization and catalytic activity of gold nanoparticles synthesized by autoreduction of aqueous chloroaurate ions with fumed silica, *Chem. Mater.*, 14 (2002) 1678–1684.
- [2] A. M. Alak, T. Vo-Dinh, Silver-coated fumed silica as a substrate material for surface-enhanced raman scattering, *Anal. Chem.*, 61 (1989) 656–660.
- [3] M. Fu, B. Qu, Synergistic flame retardant mechanism of fumed silica in ethylene–vinyl acetate/magnesium hydroxide blends, *Polym. Degrad. Stab.*, 85 (2004) 633–639.
- [4] Technical Information 1415: AEROSIL® and AEROPERL® Pharma Colloidal Silicon Dioxide Products.
- [5] Technical Information 1414: AEROPERL® 300 Pharma Improving the dissolution of poorly soluble APIs.
- [6] Technical Information 1341: AEROPERL® granulated fumed oxides.
- [7] Fact Sheet: AEROSIL® & SIPERNAT® – Silica as Thickeners for Personal Care, 2015 Evonik Corporation.
- [8] Industry Brochure: AEROSIL® and SIPERNAT® Silica for Personal Care.
- [9] Technical Information 1251: AEROSIL® and SIPERNAT® Silica: Versatile Raw Materials for Personal Care Formulations.

- [10] H. Kamiya, M. Iijima, Dispersion behavior control of nanoparticles and its applications, *The Micromeritics*, 55 (2012) 12–18.
- [11] H. Barthel, Surface interactions of dimethylsiloxy group–modified fumed silica, *Colloids Surf., A*, 101 (1995) 217–226.
- [12] Technical Bulletins No. 11, No. 23, Degussa Corp. Akron, OH, 1989.
- [13] T. Dabak, O. Yucel, Shear viscosity behavior of highly concentrated suspensions at low and high shear–rates, *Rheol. Acta*, 25 (1986) 527–533.
- [14] W.M. Jiao, A. Vidal, E. Papirer, J.B. Donnet, Modification of silica surfaces by grafting of alkyl chains part III. Particle/particle interactions: rheology of silica suspensions in low molecular weight analogs of elastomers, *Colloids Surf.*, 40 (1989) 279–291.
- [15] M. Chen, W.B. Russel, Characteristics of flocculated silica dispersions, *J. Colloid Interface Sci.*, 141 (1991) 564–577.
- [16] Decker, C. In *Proceedings of the 14th International Conference in organic Coating Science and Technology*, Patsis, A. V., Ed.; Technomic: Lancaster, PA (1988).
- [17] Z. W. Wicks, Jr., F. N. Jones, S. P. Pappas, D. A. Wicks, *Organic Coatings: Science and Technology*, Wiley Vol. 2 (1992) New York.
- [18] Pappas, S. Peter, *Radiation Curing, Science and Technology*, (1992) New York.
- [19] H. Yu, Q. Yuan, D. Wang, Y. Zhao, Preparation of an Ultraviolet–Curable Water–

BornePoly(urethane acrylate)/Silica Dispersion and Properties of Its Hybrid Film, *J. Appl. Polym. Sci.*, 94 (2004) 1347–1352.

[20] S.A. Khan, N. J. Zoeller, Dynamic rheological behavior of flocculated fumed silica suspensions, *J. Rheol.*, 37, (1993) 1225–1235.

[21] S. R. Raghavan, M. W. Riley, P. S. Fedkiw, S. A. Khan, Composite Polymer Electrolytes Based on Poly(ethyleneglycol) and Hydrophobic Fumed Silica: Dynamic Rheology and Microstructure, *Chem. Mater.*, 10 (1998) 244–251.

[22] S. Sun, C. Li, L. Zhang, H.L. Du, J.S. Burnell–Gray, Effects of surface modification of fumed silica on interfacial structures and mechanical properties of poly (vinyl chloride) composites, *Eur. Polym. J.*, 42 (2006) 1643–1652.

[23] Wu D, Wang X, Song Y, Jin R. Nanocomposites of poly (vinyl chloride) and nanometric calcium carbonate particles: effects of chlorinated polyethylene on mechanical properties, morphology, and rheology. *J. Appl. Polym. Sci.*, 92 (2004) 2714–2723.

[24] M. Takeuchi, G. Martra, S. Coluccian, M. Anpo, Evaluation of Hydrophilic/Hydrophobic Properties and Wettability of Oxide Surfaces, *Journal of the surface science society of Japan*, 30 (2009) 148–156.

[25] Y. Li, J. A. Yerian, S. A. Khan, P. S. Fedkiw, Crosslinkable fumed silica–based nanocomposite electrolytes for rechargeable lithium batteries, *J. Power Sources*, 161 (2006) 1288–1296.

- [26] B. A. Morrow, A. J. McFarlan, Infrared and gravimetric study of an aerosil and a precipitated silica using chemical and hydrogen/deuterium exchange probes, *Langmuir*, 7 (1991) 1695–1701.
- [27] J. P. Gallas, J. C. Lavalley, Comparative Study of the Surface Hydroxyl Groups of Fumed and Precipitated Silicas. 4. Infrared Study of Dehydroxylation by Thermal Treatments, *Langmuir*, 7 (1991) 1235–1240.
- [28] A. Burneau, O. Barres, J. P. Gallas, J. C. Lavalley, Comparative study of the surface hydroxyl groups of fumed and precipitated silicas. 2. Characterization by infrared spectroscopy of the interactions with water, *Langmuir*, 6 (1990) 1364–1372.
- [29] P.K. Jal, S. Patel, B.K. Mishra, Chemical modification of silica surface by immobilization of functional groups for extractive concentration of metal ions, *Talanta* 62 (2004) 1005–1028.
- [30] S. K. Parida, S. Dash, S. Patel, B.K. Mishra, Adsorption of organic molecules on silica surface, *Adv. Colloid Interface Sci.*, 121 (2006) 77–110.
- [31] M. Sabzi, S.M. Mirabedini, J. Zohuriaan-Mehr, M. Atai, Surface modification of TiO₂ nanoparticles with silane coupling agent and investigation of its effect on the properties of polyurethane composite coating, *Organic Coatings*, 65 (2009) 222–228.
- [32] <https://www.aerosil.com/product/aerosil/ja/about/pages/default.aspx>
- [33] Z. C Orel, Characterisation of high-temperature-resistant spectrally selective paints for solar absorbers, *Solar Energy Materials & Solar Cells*, 57 (1999) 291–301.

- [34] S. A. El-Gizawy, M. A. Osman, M. F. Arafa, G M. El Maghraby, Aerosil as a novel co-crystal co-former for improving the dissolution rate of hydrochlorothiazide, *Int. J. Pharm.*, 478 (2015) 773–778.
- [35] J. B. Brito, T. M. H. Costa, F. S. Rodembusch, N. M. Balzaretto, Photoluminescence of silica monoliths prepared from cold sintering of nanometric aerosil precursors under high pressure, *J. Lumin.*, 187 (2017) 154–159.
- [36] X. Li, H. Peng, B. Tian, J. Gou, Q. Yao, X. Tao, Preparation and characterization of azithromycin – Aerosil 200 solid, *Int. J. Pharm.*, 486 (2015) 175–184.
- [37] S. Khandavalli, J. P. Rothstein, Ink transfer of non-Newtonian fluids from an idealized gravure cell: The effect of shear and extensional deformation, *J. Non-Newtonian Fluid Mech.*, 243 (2017) 16–26.
- [38] A. Aguilar-Rios, P. J. Herrera-Franco, A. de J. Martínez-Gómez, A. Valadez-González, Improving the bonding between henequen fibers and high density polyethylene using atmospheric pressure ethylene-plasma treatments, *eXPRESS Polym. Lett.*, 8 (2014) 491–504.
- [39] T. Kojima, J. A. Elliott, Incipient Flow Properties of Two-Component Fine Powder Mixtures: Changing the Flowability of Smaller Particles, *AIP Conference Proceedings* 1542 (2013) 999–1002.
- [40] AEROSIL® –Fumed Silica Technical Overview, p16
- [41] AEROSIL® –Fumed Silica Technical Overview, p17

- [42] AEROSIL® –Fumed Silica Technical Overview, p51
- [43] AEROSIL® –Fumed Silica Technical Overview, p54
- [44] AEROSIL® –Fumed Silica Technical Overview, p20
- [45] https://www.silicone.jp/catalog/pdf/SilaneCouplingAgents_J.pdf.
- [46] https://www.silicone.jp/products/type/silane/detail/silane_coupling/index.shtml.
- [47] Y. Xie, C. A.S. Hill, Z. Xiao, H. Militz, C. Mai, Silane coupling agents used for natural fiber/polymer composites, *Composites Part A*, 41 (2010) 806–819.
- [48] C. Y. K. Lung, J. P. Matinlinna, Aspects of silane coupling agents and surface conditioning in dentistry: An overview, *Dent. Mater.*, 28 (2012) 467–477.
- [49] <https://www.silicone.jp/products/type/silanecoup/index.shtml>.
- [50] Particle technology meeting The volume, Particle technology series The 5th reel, functionalisation by organization control of powder particle, Nikkankogyo Shinbun Co., (2008), Japan.
- [51] *Organic Solvents* 4th Ed, John Wiley & Sons (1986).
- [52] M. fuji, H. Iwata, T. Takei, T. Watanabe, M. Chikazawa, The change in the water vapor affinity of fine particles loaded with trimethylsilyl Groups, *J. Soc. Powder Technol., Japan*, 32 (1995) 649–654.
- [53] M. Fuji. T. Takei. T. Watanabe, C. Chikazawa, Wettability of fine silica powder surfaces modified with several normal alcohols, *Colloids Surf., A*, 154 (1999) 13–24.

- [54] J. Feng, D. Chen, W. Ni, S. Yang, Z. Hu, Study of IR absorption properties of fumed silica-opacifier composites, *Journal of Non-Crystalline Solids*, 356 (2010) 480–483.
- [55] E.F. Voronin, V.M. Gun'ko, N.V. Guzenko, E.M. Pakhlov, L.V. Nosach, R. Leboda, J. Skubiszewska-Zieba, M.L. Malysheva, M.V. Borysenko, A.A. Chuiko, Interaction of poly(ethylene oxide) with fumed silica, *J. Colloid Interface Sci.*, 279 (2004) 326–340.
- [56] K. Chrissafis, K.M. Paraskevopoulo, E. Pavlidoua, D. Bikiaris, Thermal degradation mechanism of HDPE nanocomposites containing fumed silica nanoparticles, *Thermochimica Acta*, 485 (2009) 65–71.
- [57] R. M. Mohame, H. M. Aly, M. F. El-Shahat, I. A. Ibrahim, Effect of the silica sources on the crystallinity of nanosized ZSM-5 zeolite, *Microporous Mesoporous Mater.*, 79 (2005) 7–12.
- [58] V. V. Brei, ^{29}Si solid-state NMR study of the surface structure of aerosil silica, *Journal of the Chemical Society, Faraday Trans.*, 90 (1994) 2961–2964.
- [59] H. Hamdan, M. N. M. Muhid, S. Endud, E. Listiorini, Z. Ramli, ^{29}Si MAS NMR, XRD and FESEM studies of rice husk silica for the synthesis of zeolites, *J. Non-Cryst. Solids*, 211 (1997) 126–131.
- [60] A. Tuel, H. Hommel, A. P. Legrand, A ^{29}Si NMR Study of the Silanol Population at the Surface of Derivatized Silica, *Langmuir*, 6 (1990) 770–775.
- [61] A. Tuel, H. Hommel, A. P. Legrand, Y. Chevallier, J. C. Morawski, Solid state NMR studies of

precipitated and pyrogenic silicas, *Colloids and Surfaces*, 45 (1990) 413–426.

[62] K. Kato, A. Ueda, K. Shimizu, Investigation on silica powder recovered from geothermal brines as an admixtures of high strength ceramics, *Shigen-to-Sozai*, 119 (2003) 71–78.

[63] V. M. Gun'ko, V. I. Zarko, V. V. Turov, R. Leboda, E. Chibowski, E. M. Pakhlov, E. V. Goncharuk, M. Marciniak, E. F. Voronin, A. A. Chuiko, Characterization of Fumed Alumina/Silica/Titania in the Gas Phase and in Aqueous Suspension, *J. Colloid Interface Sci.*, 220 (1999) 302–323.

[64] V. M. Gun'koa, V. I. Zarkoa, R. Lebodab, E. Chibowski, Aqueous suspension of fumed oxides: particle size distribution and zeta potential, *Adv. Colloid Interface Sci.*, 91 (2001) 1–112.

Chapter 2: Effect of solvent polarity and adsorbed water on reaction between hexyltriethoxysilane and fumed silica

2-1. Introduction

Nano-sized fumed silica is widely used in many fields such as cosmetics [1, 2], CMP and electronics [3], sealants and adhesives [4–6], paints and coatings [7–10], silicone rubbers [11], and toners [12] to improve their functionalities. For these applications, dispersion of fumed silica in the desired medium, such as organic solvents, polymers, and water, is required. However, fumed silica easily aggregates owing to the hydrophilic silanol (SiOH) groups on its surface [13]. To obtain uniform dispersion in organic solvents, the affinity between the silica surface and solvent is effectively controlled through surface modification using modifiers such as silane coupling agents and alcohols [14, 15].

Silane coupling agents mostly have one type of functional group, which can be hydrophobic, hydrophilic, polar, or non-polar. The other groups are alkoxide (OR), which turns into SiOH via hydrolysis in the presence of water and then forms hydrogen bonds with the SiOH groups of the silica surface. The functional groups of the modifier should be compatible for the organic solvent. The reaction between the modifiers and the silica surface can occur in gas phase [16, 17], liquid phase [17, 18], and by autoclaving [19]. In the liquid phase, the modifier is dissolved in the selected organic solvent and is followed by hydrolysis and condensation aided by heating or the addition of a catalyst [20].

In the liquid phase reaction, the following surface modification process can occur:

- a) The modifier undergoes hydrolysis to form the SiOH group.
- b) The hydrolyzed modifier forms hydrogen bonds between its SiOH groups and those of the silica surface.
- c) Covalent bonds are formed by the dehydration of SiOH.

In reaction a), the water adsorbed at the silica surface facilitates the hydrolysis of the modifier; reaction b) depends on the stability of the modifier-adsorbed silica in the reaction solvents; and reaction c) is promoted by heating or the addition of a catalyst. The progress of reaction b) could be dominated by the physical properties of the selected solvent, such as their polarity, and solubility of the modifier.

Hexane and toluene are generally used as solvents for surface modification in the liquid phase [21, 22]. Since these solvents are chemically stable, there is a low probability of limiting the reaction between the modifier and silica surface.

For the hydrolysis of modifier, only a small amount of water, which is at least molar equivalent of the modifier, is necessary. As the silica surface has many SiOH groups, a certain amount of water adsorbs chemically and physically, which can be controlled by relative humidity [23]. In hexane and toluene, the adsorbed water on the silica surface could be useful for hydrolysis because the hydrophobic solvents do not absorb water from the atmosphere. Hexane and toluene are effective

reacting solvents for surface modification; however, the difference in the progress of the reaction of modifier and solvents in terms of their physical properties has not been investigated.

In this study, the effect of solvents on the surface modification progress was investigated. Fumed silica was chosen because of its non-porosity and surface smoothness, and hexane and toluene were used as low polarity solvents. For comparison, acetone was used as a high polarity solvent. Relative permittivity was used as an index for solvent polarity. In addition, hexyltriethoxysilane was used as a modifier. The relationship between the amount of adsorbed water at the silica surface and that in the reacting solvent was investigated, and the optimum water amount required for surface modification was determined.

2-2. Experimental

2-2-1. Materials

Hexane (Hex), toluene (Tol), and acetone (Ace) of special chemical grade (Wako Pure Chemical Industries, Ltd.) were used as organic solvents after overnight removal of the dissolved water by dried molecular sieves (3A Wako Pure Chemical Industries, Ltd.). Fumed silica powder was supplied by Nippon Aerosil Co., Ltd., as Aerosil200 (abbreviated A200) with the specific surface area of 200 m²/g calculated by applying the Brunauer-Emmett-Teller (BET) equation [24] to the nitrogen adsorption isotherms. To adjust the amount of water adsorbed on the A200 surface, the A200 was dried under

reduced pressure at 180 °C for 2 h then the A200 was exposed to the various relative humidities (RH) of 42.8, 68.8, and 92.0 % for one week at 25 °C by the corresponding saturated salt solutions of K₂CO₃, KI, and KNO₃ (Wako Pure Chemical Industries, Ltd.), respectively [25–28]. The amounts of water at for 2g of the A200 surface were determined to be as 30, 50, and 190 mg, respectively. As a the surface modifier agent, hexyltriethoxysilane (HTES, CH₃(CH₂)₅Si(OCH₂CH₃)₃, Tokyo Chemical Industry Co., Ltd.) with a hydrophobic chain was used.

2-2-2. Surface modification

The A200 (2.0 g) samples with the controlled adsorbed water were dispersed in the dehydrated solvents (150 ml) containing 0.3 – 4.2 ml/g of dissolved HTES. The suspensions were stored at 50 °C for 1 h. The treated A200 samples were separated by centrifugation and dried under reduced pressure at 80 °C for 2 h.

2-2-3. Characterizations

How many CH₃(CH₂)₅Si (-C₆) groups of HTES introduced on the A200 surface was determined using thermogravimetric and differential thermal analysis (TG-DTA, Thermo Plus 8120, Rigaku Co., Ltd.) as shown in Fig. 2-1.

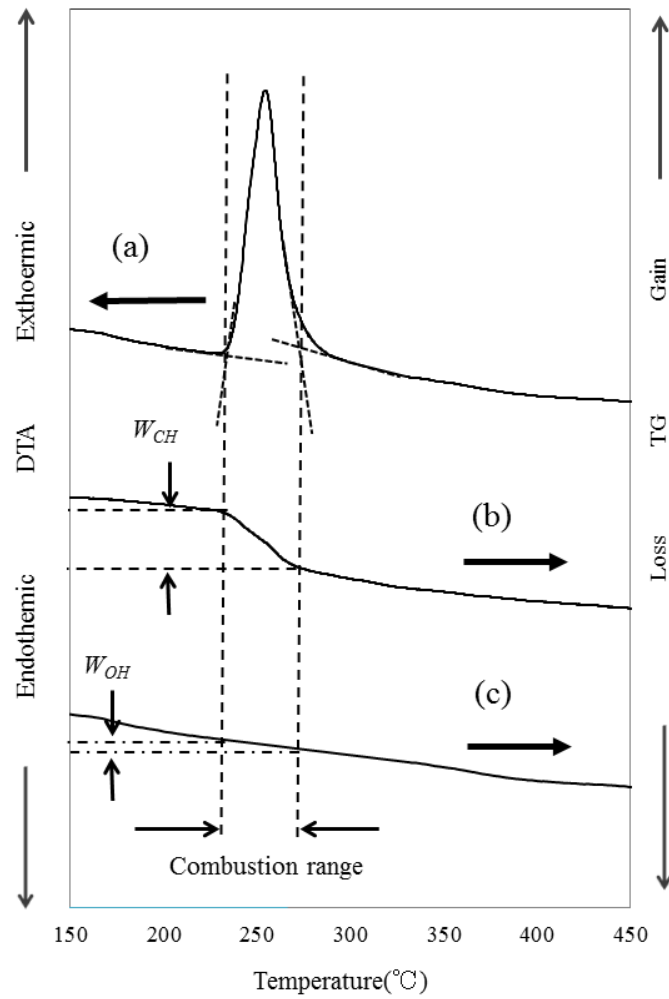


Fig. 2-1 Estimation of the number of HTES (C_6) groups introduced onto the A200 surface from thermogravimetric analysis (TG) differential thermal analysis (DTA) (a) DTA curve for modified A200, (b) TGA curve for modified silica, (c) TGA curve for unmodified A200.

The measurement was carried out under air. The value was calculated from the difference in the weight loss between modified sample (W_{CH}) and unmodified sample (W_{OH}). Described as the surface

HTES density were determined by the following equation (1) [29, 30].

$$d_A (-C_6/nm^2) = \frac{(\Delta W_{CH} - \Delta W_{OH}) N_A}{M_W S_{N_2}} \times 10^{-18} \quad (1)$$

where d_A is the surface density ($-C_6/nm^2$), M_w is the the molecular weight of the modifier, S_{N_2} is the BET specific surface area measured from the nitrogen adsorption isotherm, and N_A is Avogadro's number. ΔW_{CH} and ΔW_{OH} are the weight loss of the modified and unmodified A200 measured by thermogravimetric and differential thermal analyze, respectively.

2-3. Results and discussion

To investigate the effect of solvent polarity on the surface HTES density, the A200 sample with 30 mg of adsorbed water was treated in each solvent at 50 °C for 1 h. The relative permittivities (ϵ/ϵ_0) of Hex, Tol, and Ace were 1.88, 2.38, and 20.7, respectively [32, 33]. Fig. 2-2 shows the surface HTES density as a function of the added amount of HTES from 0.3 to 4.2 ml/g in (a) Hex, (b) Tol, and (c) Ace. It is evident that the surface HTES density increased with increasing ϵ/ϵ_0 (Hex < Tol < Ace). In Hex, the surface HTES density is almost constant at about 0.3 ($-C_6/nm^2$) over the entire range of added HTES, while in Tol, it increased with increase in the HTES amount. In Ace, the surface HTES density was low and constant at about 0.1- C_6/nm^2 .

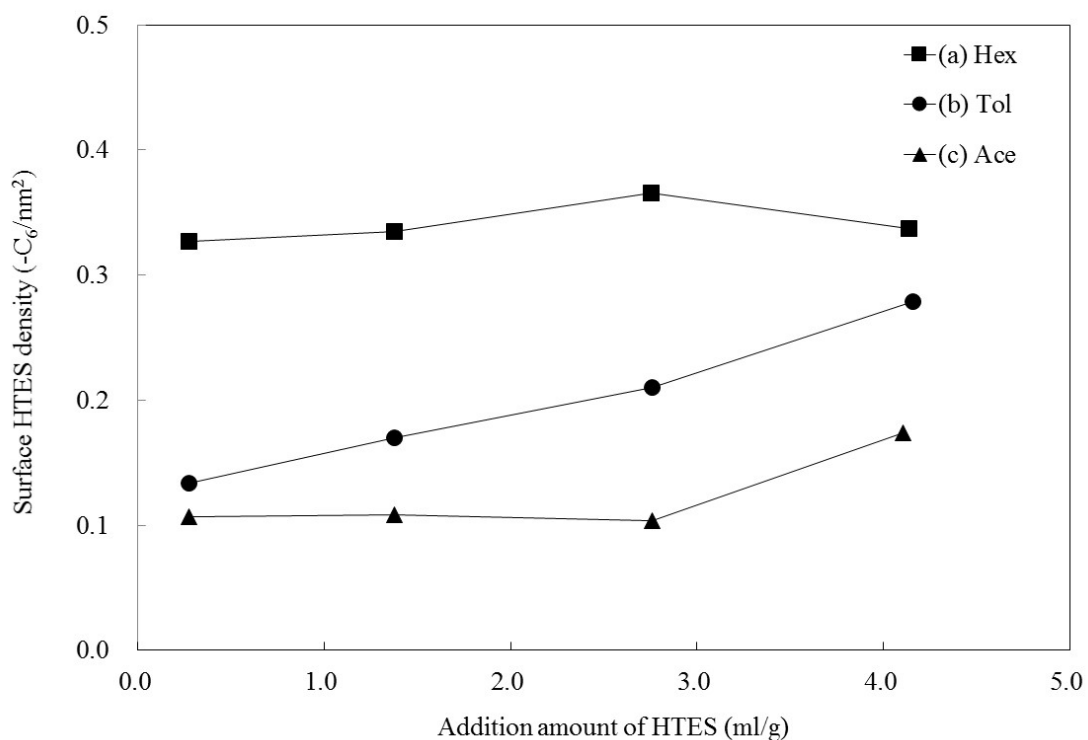


Fig. 2-2 Surface HTES density in (a) Hex, (b) Tol, and (c) Ace as a function of added HTES amount.

Since Ace is a polar solvent, it does not promote the reaction of HTES with the non-polar C₆ group and the polar A200 surface. Tol and Hex, being non-polar, are categorized as hydrophobic solvents, and hence, the affinity of A200 for both Tol and Hex is low. HTES molecules can work as stabilizers for A200 by adsorbing on its surface. However, the behavior of the surface HTES density with the added HTES amount is entirely different, as observed from Fig. 2-2.

The following reactions are involved in the surface modification process: a) hydrolysis of HTES to form silanol (SiOH) groups, b) hydrogen bond formation between the SiOH groups of the hydrolyzed HTES and that of the A200 surface, and c) dehydration of the SiOH groups to form

covalent bonds. In reaction a), the water adsorbed at the A200 surface participates in the hydrolysis of HTES; reaction b) depends on the stability of A200 by the adsorption of HTES in the reaction solvents; and reaction c) is promoted by heating [34–37].

The physical properties of the solvents affect the progress of reaction b). Apart from ϵ/ϵ_0 , the solubility of HTES in the solvents was determined. In a good solvent, HTES can easily approach the A200 surface; that is, the solubility parameters (SP) of HTES and the solvents should be close. Table 2-1 shows the SP values of Hex and Tol and the difference between the SP values of the solvents and HTES before and after hydrolysis.

Table 2-1. (a) Solubility parameter (SP) of Hex and Tol, (b) SP difference between solvents and HTES, and (c) SP difference between solvent and hydrolyzed HTES [30].

Solvent	(a) Solubility Parameter (SP)	(b) $\Delta\sigma (\text{C}_2\text{H}_5\text{O})_3\text{SiC}_6\text{H}_{12}$	(c) $\Delta\sigma (\text{OH})_3\text{SiC}_6\text{H}_{12}$
Hexane	7.28	0.63	5.11
Toluene	9.14	1.23	3.25

The SP value difference between Hex and HTES is as low as 0.63, while that for Tol and Ace, it is 1.23 and 1.26, respectively, which is two times higher than that of Hex. The solubility power of Tol is lower than that of Hex, possibly because of the pi-bond in Tol, which is absent in HTES. On the other hand, the solubility of the hydrolyzed HTES significantly deteriorates in Hex and is low in Tol and Ace because of the polar SiOH groups in the HTES molecules.

The adsorbed water at the A200 surface corresponding to the RH of 42.8 % is 30 mg; this amount

appears to be sufficient for the hydrolysis of 0.3 ($-C_6/nm^2$) HTES at the A200 surface (Fig. 2-2(a)). The adsorbed water can adhere as a layer on the A200 surface in Hex because of Hex's hydrophobicity. HTES tends to stabilize the polar A200 surface in Hex by adsorbing through the alkoxy groups. After the alkoxy groups of HTES attach to the adsorbed layer on the A200 surface, the hydrolyzed HTES forms hydrogen bond with the A200 surface. The lowest added amount of 0.3 ml/g of HTES (Fig. 2-2) corresponds to 2.8 SiOH/ nm^2 on the A200 surface [30]. However, the actual surface HTES density was 0.3 ($-C_6/nm^2$), which could be due to the steric hindrance of the C_6 groups of the modified HTES.

Unlike Hex, Tol has a low water miscibility of 0.067 wt% (at 23.5 °C) [38]. Therefore, the adsorbed water layer on the A200 surface forms a "diffused layer" in Tol near the A200 surface. The solubility of HTES without the pi-bond is relatively low in Tol than in Hex. Despite this, HTES acts as a stabilizer for A200 in Tol. When HTES reaches the diffused layer, it undergoes stepwise hydrolysis with a small amount of water. Because the solubility of the hydrolyzed HTES in Tol is low, it moves toward the silica surface to form hydrogen bonds. Thus, the increase in surface HTES density with increase in HTES amount (Fig. 2-2(b)) can be ascribed to the low solubility of HTES in Tol [39].

Since these factors affect the progress of surface modification, the amount of adsorbed water on the A200 surface can be determined. The effects of the adsorbed water amount on the surface HTES density in Hex or Tol were investigated. Fig. 2-3 shows the surface HTES density of 42.8–90.0% RH-controlled A200 in (a) Hex and (b) Tol.

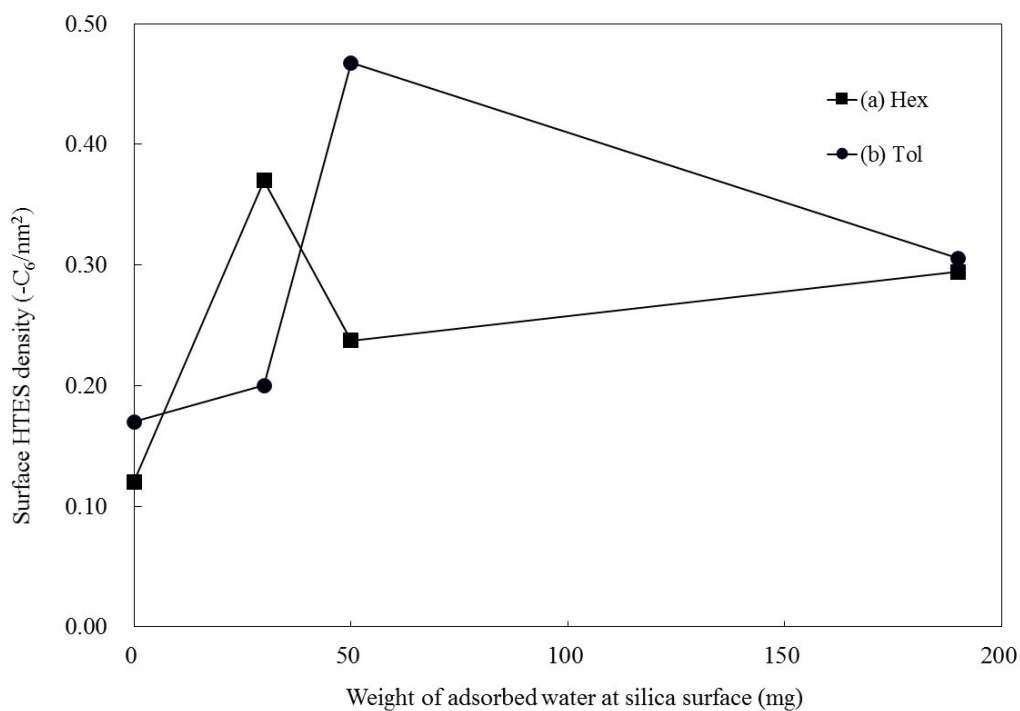


Fig. 2-3 Effects of various weights of adsorbed water on silica surface which were controlled at RH of 42.8, 68.8, and 90.0 % for A200 reacted in (a) Hex and (b) Tol on surface HTES density.

The reaction was conducted at 50 °C for 1 h. Here, 0 mg represents the modified A200 without RH control just after drying under reduced pressure at 180 °C for 2 h. It seems that the weight of the adsorbed water, which provides the maximum surface HTES density, is different in Tol and Hex. In Hex, the surface HTES density is 0.12 ($-C_6/\text{nm}^2$) without RH control, and attains a maximum value of 0.37 ($-C_6/\text{nm}^2$) with 30 mg adsorbed water. Thereafter, it decreases to 0.20 ($-C_6/\text{nm}^2$) with further increase in the weight of adsorbed water to 190 mg. However, in Tol, the surface HTES density

remained almost constant at 0.17 ($-C_6/\text{nm}^2$) with an increase in the weight of adsorbed water for up to 30 mg; it then reached a maximum value of 0.47 ($-C_6/\text{nm}^2$) at 50 mg of adsorbed water and then decreased.

As already described, 30 mg adsorbed water seems to be enough for the hydrolysis of 0.3 ($-C_6/\text{nm}^2$) HTES. With an increase in the weight of adsorbed water, the thickness of the “adsorbed water layer” on the A200 surface in Hex seems to increase. The hydrophilicity of A200 with a thick water layer increases and the affinity with Hex becomes low. The alkoxy groups of HTES approach the “adsorbed water layer” on the A200 surface and are hydrolyzed. However, the hydrolyzed HTES could not contact the A200 surface due to the thick “adsorbed water layer.” Additionally, the solubility of the hydrolyzed HTES in Hex is low, which prevented its hydrolysis and modification.

The adsorbed water layer on the A200 surface is diluted by Tol. Therefore, to hydrolyze HTES, which reaches the “diffused water layer” of A200, more than 30 mg of water is required. It is estimated that 50 mg could be the proper amount. With increase in the weight of adsorbed water, the diffused layer thickness increases. Similar to the reaction in Hex, the solubility of hydrolyzed HTES in Tol is low, and the thick water layer prevents the HTES from approaching the A200 surface. Therefore, the surface modification of HTES is not promoted in Tol, as shown in Fig. 2-3(b).

Zheng Yang reported that preferential adsorption of Tol vapor on the silica surface occurs when silica is exposed to a mixture of Tol and Hex vapors due to the interaction of the pi-bond in the Tol

molecules with the SiOH groups on the silica surface [40]. In this experiment, the effect of Tol on the diffused water layer on the A200 surface was investigated. Fig. 2-4 shows the surface HTES density of A200 prepared in different Hex/Tol mixtures with 100/0, 75/25, 50/50, 25/75, and 0/100 v/v ratios.

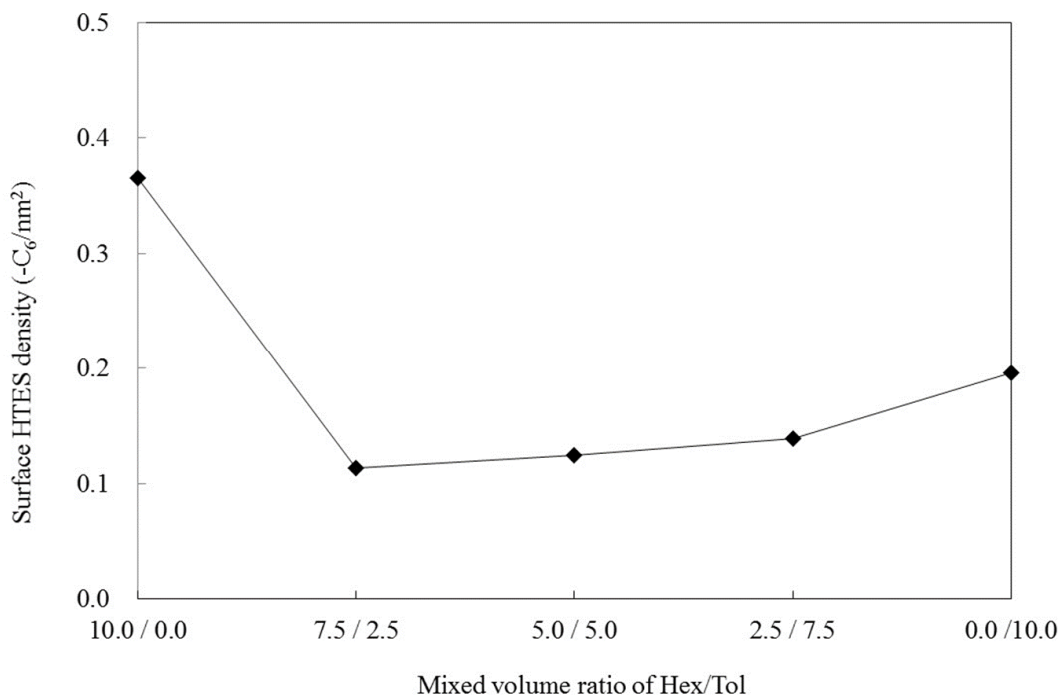


Fig. 2-4 Effects of different Hex/Tol volume ratios of 100/0, 75/25, 50/50, 25/75, and 0/100 on surface HTES density.

The adsorbed water on A200 was controlled at 42.8 % RH and reacted at 50 °C for 1 h; thus, the HTES amount was selected as 3.0 ml/g.

In Hex (100/0), the surface HTES density was 0.37 ($-C_6/\text{nm}^2$), which decreased to 0.11 ($-C_6/\text{nm}^2$) for Hex/Tol = 75/25. With an increase in the Tol ratio, the surface HTES density remained almost constant at around 0.11 ($-C_6/\text{nm}^2$), though with a slight increase. In Tol (0/100), the surface HTES

density was $0.20 (-C_6/nm^2)$. These results clearly indicate that Tol prevents the progress of the reaction between HTES and A200.

The adsorption of Tol on the A200 surface due its presence in the reaction media was investigated. A certain amount of Tol was added to Hex in which A200 was dispersed. The suspension was heated at $50\text{ }^\circ\text{C}$ for 1 h in the same way as in the surface modification process. Based on gas chromatography and mass spectroscopy (GC-MS) analysis, the adsorption of Tol on the A200 surface was confirmed at $300\text{ }^\circ\text{C}$.

As already described, in Hex, the hydrolysis of HTES occurs when HTES reaches the water adsorbed “layer” of A200. When Tol was added to Hex at 75/25, Tol approaches the water layer due to its slight water miscibility to form a “diffused layer.” It can thus be said that A200 with a diffused layer was dispersed in the Hex/Tol mixture. Tol molecules in the diffused layer gradually approach the A200 surface and adsorb at the SiOH groups of A200, which prevents HTES from forming hydrogen bonds with the SiOH groups of A200. In addition, HTES before hydrolysis dissolves in a sufficient amount of Hex in the mixture; therefore, the hydrolysis of HTES is not promoted, and consequently, the surface HTES density decreases.

Even if the Tol ratio increases (50/50 and 25/75), the thickness of the diffused layer does not remarkably change, and the surface HTES density does not increase. In Tol (0/100), the solubility of HTES before hydrolysis is low; here, HTES is hydrolyzed by the water in the diffused water layer of

A200 than by dissolving in Tol. Consequently, the surface HTES density in Tol increases compared to that in the Hex/Tol mixture.

2-4. Conclusion

The effects of the physical properties of a solvent and the amount of adsorbed water on the A200 surface on the surface HTES density were investigated.

1. With an increase in solvent polarity (Hex < Tol < Ace), the surface HTES density decreased. The difference in the surface HTES density in Hex and Tol, which have similar polarities, is due to the low solubility of HTES in Tol.
2. The maximum surface HTES densities in Hex and Tol with different RHs were 42.8 % (weight of adsorbed water is 30 mg) and 68.8 % (weight of adsorbed water is 50 mg), respectively. In Hex, the water adsorbs as a “layer” on the A200 surface, while in Tol, water forms a “diffused layer.” For the hydrolysis of HTES, more water was required in Tol than in Hex.
3. Tol in the diffused layer tends to adsorb at the SiOH groups of A200. Therefore, HTES cannot approach the A200 surface and the reaction between HTES and A200 is not promoted.

Based on these results, in addition to the difference in ϵ/ϵ_0 between the modifier and solvent, the solubility of the modifier in the solvent before and after hydrolysis and the amount of water adsorbed at the particle surface should be considered to control the progress of surface modification.

References

- [1] A. Jaroenworarluck, N. Pijarn, N. Kosachan, R. Stevens, Nanocomposite TiO₂-SiO₂ gel for UV absorption, *Chem. Eng. J.* 181–182, (2012) 45–55.
- [2] L. Forny, K. Saleh, I. Pezron, L. Komunjer, P. Guigon, Influence of mixing characteristics for water encapsulation by self-assembling hydrophobic silica nanoparticles, *Powder Technol.* 189, (2009) 263–269.
- [3] Y. Kang, Y.N. Prasad, I. Kim, S. Jung, J. Park, Synthesis of Fe metal precipitated colloidal silica and its application to W chemical mechanical polishing (CMP) slurry, *J. Colloid Interface Sci.* 349 (2010) 402–407.
- [4] B. Jaúregui-Beloqui, J.C. Fernández-García, A.C. Orgilés-Barceló, M.M. Mahiques-Bujanda, J.M. Martín-Martínez, Rheological properties of thermoplastic polyurethane adhesive solutions containing fumed silicas of different surface areas, *Int. J. Adhes. Adhes.* 19 (1999) 321–328.
- [5] J. Paquien, J. Galy, J. Gérard, A. Pouchelon, Bonding strength and water resistance of starch-based wood adhesive improved by silica nanoparticles, *Colloids Surf., A*: 260 (2005) 165–172.
- [6] J. Comyn, F. de Buyl, T.P. Comyn, Diffusion of adhesion promoting and crosslinking additives in an uncured silicone sealant, *Int. J. Adhes. Adhes.* 23, (2003), 495–497.
- [7] M. Rostami, Z. Ranjbar, M. Mohseni, Investigating the interfacial interaction of different aminosilane treated nano silicas with a polyurethane coating, *Appl. Surf. Sci.* 257 (2010) 899–904.

- [8] T. Mizutani, K. Arai, M. Miyamoto, Y. Kimura, Application of silica-containing nano-composite emulsion to wall paint: A new environmentally safe paint of high performance, *Prog. Org. Coat.* 55 (2006) 276–283.
- [9] M.M. Jalili, S. Moradian, Deterministic performance parameters for an automotive polyurethane clearcoat loaded with hydrophilic or hydrophobic nano-silica, *Prog. Org. Coat.* 66 (2009) 359–366
- [10] F. Bauer, R. Flyunt, K. Czihal, H. Langguth, R. Mehnert, R. Schubert, M.R. Buchmeiser, UV curing and matting of acrylate coatings reinforced by nano-silica and micro-corundum particles, *Prog. Org. Coat.* 60 (2007) 121–126.
- [11] I Stevenson, L David, C Gauthier, L Arambourg, J Davenas, G Vigier, Influence of SiO₂ fillers on the irradiation aging of silicone rubbers, *Polym. J.* 42 (2001) 9287–9292
- [12] H. Zhang, W. Ding, K. Law, C. Cetinkaya, Adhesion properties of nanoparticle-coated emulsion aggregation toner, *Powder Technol.* 208 (2011) 582–589.
- [13] S. Ek, A. Root, M. Peussa, L. Niinistö, Determination of the hydroxyl group content in silica by thermogravimetry and a comparison with MAS NMR results, *Thermochim. Acta*, 379 (2001) 201–212.
- [14] D. An, Z. Wang, X. Zhao, Y. Liu, Y. Guo, S. Ren, A new route to synthesis of surface hydrophobic silica with long-chain alcohols in water phase, *Colloids Surf., A*: 369, (2010) 218–222.
- [15] M. Fuji, S. Ueno, T. Takei, T. Watanabe, M. Chikazawa, Surface structural analysis of fine silica

powder modified with butyl alcohol, *Colloid. Polym. Sci.* 278 (2000) 30–36.

[16] Y. Ouabbas, A. Chamayou, L. Galet, M. Baron, G. Thomas, P. Grosseau, B. Guilhot, Surface modification of silica particles by dry coating: Characterization and powder aging, *Powder Technol.* 190 (2009) 200–209.

[17] B. Prélot, S. Lantenois, Y. Nedellec, M. Lindheimer, J.M. Douillard, J. Zajac, The difference between the surface reactivity of amorphous silica in the gas and liquid phase due to material porosity, *Colloids Surf., A*, 355 (2010) 67–74.

[18] S. Sun, C. Li, L. Zhang, H.L. Du, J.S. Burnell-Gray, Effect of surface modification of fumed silica on interfacial structure and mechanical properties of poly(vinyl chloride) composite, *Eur. Polym. J.* 42 (2006) 1643–1652.

[19] C. Takai, M. Fuji, M. Takahashi, A novel surface designed technique to disperse silica nano particle into polymer, *Colloids Surf., A*, 292 (2007) 79–82

[20] T.M. Chen, G.M. Brauer, Solvent effect on bonding organo-silane to silica surface, *J. Dent. Res.* 61 (1982) 1439–1443.

[21] J.W. Park, Y.J. Park, C. Jun, Post-grafting of silica surfaces with pre-functionalized organosilanes: new synthetic equivalents of conventional trialkoxysilanes, *Chem. Commun.*, 47 (2011) 4860–4871.

[22] E. Ido, K. Kakiage, T. Kyomen, M. Hanaya, A new method of silica coupling treatment: Chemical surface modifications of metal oxide with hydrosilane, *Chem. Lett.* 41 (2012) 853–854.

- [23] A. Kawamura, C. Takai, M. Masayoshi, T. Shirai, Effect of Water Adsorption on Dispersibility of Fumed Silica in Mixed Organic Solvent of Ethanol and Hexane, *J. Soc. Powder Technol.(Jpn.)* 48 (2011) 755–760.
- [24] S. Brunauer, P. H. Emmett, E. Teller, Adsorption of gases in multimolecular layers, *J. Am.*, 60 (1938) 309–319.
- [25] Japan macromolecule and moisture absorption committee, *Ingredient and water handbook: Moisture absorption, moisture proof, moisture conditioning and dryness*, first ed., Society of Polymer Science, Tokyo, 1968.
- [26] Stokes, R. H. and R. A. Robinson: Standard solution for humidity control at 25°C, *Ind. Eng. Chem.*, 41 (1949) 2013.
- [27] Acheson, D. T.: Vapor pressure of saturated aqueous salt solutions, *Humidity and Moisture*, 3, (1965) 521.
- [28] Wexler, A. and S. Hasegawa: Relative humidity-temperature relationships of some saturated salt solutions in the temperature range 0° to 50°C, *J. Res. Nat. Bur. Stand*, 53 (1954) 19.
- [29] M. Fuji, C. Takai, Y. Tarutani, T. Takai, M. Takahashi, Surface properties of nanosize hollow silica particles on the molecular level, *Adv. Powder Technol.* 18 (2007) 81–91.
- [30] M. Fuji, H. Iwata, T. Takei, T. Watanabe, M. Chikazawa, The change in the water vapor affinity of fine silica particles loaded with trimethylsilyl groups, *Adv. Powder Technol.* 8 (1997) 325–334.

- [31] Y. Setsuko, K. Shigetoshi, F. Kenji, S. Yusuke, A. Yasuhiko, Prediction method of solubility parameter based on molecular structure, *J. Assoc. Mater. Eng. Res.* 19 (2006) 25–27.
- [32] *Organic Solvents* 4th ed, John Wiley & Sons (1986).
- [33] *Kagaku Binran Kisihen*, ed. by The Chemical Society of Japan, Maruzen, Tokyo, (2004).
- [34] H. Utsugi, N. Suzuki, Surface Modification of Fine Powders and the Reactivity of the Surface Groups - The Surface-treatment of the Silica Gels with Organo-Silyl Chlorides and the Chemical Properties of their Surface Groups, *J. Soc. Powder Technol.*, 20 (1983) 744–751.
- [35] H. Kamiya, M. Iijima, Dispersion Behavior Control of Nanoparticles and its Applications, *The Micromeritics*, 55 (2012) 12–18.
- [36] T. Murakawa, Trends of surface modification of aluminum, *J. Jpn. Inst. Light Met.*, 38 (1988) 485-495.
- [37] M. Koishi, Surface Modification and Dispersion of Pigment, *JSCM*, 51 (1978) 473–481.
- [38] *The Merck Index* 13th (2001) Merck Co., Inc.
- [39] M. Sando, A. Towata, A. Tsuge, Nano-Meter Level Coating on Potassium Titanate Whisker, *KAGAKU KOGAKU RONBUNSHU*, 18 (1992) 308–314.
- [40] Z. Yang, Q. Li, R. Hua, M.R. Gray, K.C. Chou, Competitive adsorption of toluene and n-alkanes at binary solution/silica interfaces, *J. Phys. Chem.* 113 (2009) 20355–20359.

Chapter 3: Effect of steric hindrance on surface wettability of fine silica powder modified by *n*- or *t*-butyl alcohol

3-1. Introduction

Fumed silica is a unique industrial material owing to its extremely small particle size, large surface area, and high purity [1]. Fumed silica is widely used in medical products as a glidant [2], in cosmetics as a sun protection agent [3], in electronics for chemical-mechanic planarization (CMP) [4,5], in paints and printing inks as a thickening agent [6–8], an anticaking agent in the processing of dry materials, and in thermal insulators for high temperatures (~1000 °C). Another important industrial use of the fumed silica powder is as a filler. Silica fillers are key materials used for reinforcing the high-performance / high-functional industrial products [9,10]. Thus, recently, high performance fillers that can meet diverse industrial requirements are desired. Nanosized silica fillers have an advantage over their micrometer or millimeter-sized counterparts owing to their high surface area, which leads to better reactivity and adhesion between the filler and matrix particles. However, nanosized silica particles usually suffer from aggregation [11–13], which is nanosized particles tend to stick to each other due to the high surface area. Therefore, the development of monodisperse silica nanoparticles that hardly aggregate is of great importance for both industrial and academic applications.

Another factor that causes the aggregation of silica particles is hydroxyl groups (–OH) that are present on the surface of fumed silica particles [1]. These hydroxyl groups can be in the form of isolated hydroxyl groups, hydrogen-bonded hydroxyl groups, geminal hydroxyl groups, and siloxane

groups, which usually facilitate the aggregation of silica particles. Therefore, the surface of silica particles is usually modified by various functional groups such as alcohol [14,15], silane coupling agents [16–18], and silicone oil [19,20] in order to prevent their aggregation. Determining the degree of modification is also important and evaluation methods such as measuring the weight loss by thermogravimetric and differential thermal analysis (TG-DTA) [11,15], examining the wettability by preferential dispersion test [15], measuring total organic carbon content [1], and measuring the contact angle between the silica surface and water [21,22] have been reported. However, to the best of our knowledge, a systematic study, which investigates the interaction of water molecules and modifiers present on the surface of silica particles is lacking. Moreover, molecular level understanding of the surface structure of modified silica particles is important for improving the performance of silica nanoparticles, i.e., the wettability of a fumed silica surface is dependent on the molecular structure of the functional species on the surface of silica particles [23].

Fourier transform infrared spectroscopy (FT-IR) has been widely used for the observation of fumed silica surfaces and the states of their hydroxyl groups [24]. However, a comparison between the macroscopic and microscopic results will help obtain a better view of the surface wettability of modified fumed silica. In the present study, the wettability of fumed silica surfaces modified by two different structures of butyl alcohol is measured. Here, the preferential dispersion test in water is used as the macroscopic wettability evaluation method, while the water vapor adsorption test determined

by FT-IR is used as the microscopic wettability evaluation method. Finally, a molecular level mechanism for the formation of a water film on the surface of silica is proposed.

3-2. Experimental

3-2-1 Materials

Fumed silica powder (Aerosil 200, A200) is provided by Nippon Aerosil Co., Ltd. The specific surface area ($200 \text{ m}^2/\text{g}$) is measured using the Brunauer-Emmett-Teller (BET) method by nitrogen adsorption isotherms [25]. *n*- and *t*-butyl alcohols (special chemical grade, Kanto Chemical Co., Inc.) are used as modifying agents, and *n*-hexane is used as solvent.

3-2-2 Surface modification

Surface modification of the fumed silica is carried out using the autoclave [26, 27]. 2.0 g of A200 sample is dispersed in *n*-hexane containing 0–1.4 ml/g of either *n*- or *t*-butyl alcohol. The samples are dispersed in *n*-hexane and placed in the autoclave system. Autoclave system is purged by N_2 gas for 5 min to completely remove the air. Finally, the system is heated at 260°C for 1 h at 30 bar.

3-2-3 Characteristics of silica surface

The proportion of butoxy groups introduced onto the silica particles is determined by

thermogravimetry-differential thermal analysis (TG-DTA; TG/DTA300 SSC 5200H, Seiko Instrument, Inc.). Measurements are conducted in air flow of 250 ml/min at up to 500 °C with a heating ramp of 20 °C/min. The modification ratio of butoxy groups θ (%) on the silica surface is calculated using the following equation:

$$\theta (\%) = \frac{(\Delta G/y_3 - w) \times N_A}{mw \times S \times N_{OH}} \times 100 \quad (1)$$

where ΔG is the weight loss of the modified sample measured by TG-DTA, y_3 is the initial weight of the modified sample, w is the weight loss of surface silanol groups from unmodified silica, mw is the molar weight of the species used for modification, S is the BET specific surface area calculated from the nitrogen adsorption isotherm, N_A is Avogadro's number, and N_{OH} is the surface silanol density (-OH/m²) [11, 28].

The extent of silica surface modification is also observed using FT-IR (IR 5300, Jasco Corporation; operated at a resolution of 2 cm⁻¹ and with 16 scans per spectrum). The modified samples are molded and placed into a sample cell. The system is depressurized to 10⁻¹ Pa, and the sample is pretreated by degassing at 160 °C. FT-IR spectra are quantitatively analyzed. Absorbance at 1864 cm⁻¹ is used as the standard peak because it is reported to be proportional to the thickness of the sample pellet [29]. The absorbance of the modifiers is examined in the range of 2800–3000 cm⁻¹.

3-2-4 Determination of the amount of water vapor adsorption by FT-IR

The microscopic wettability of modified silica is determined by measuring water vapor adsorption using FT-IR [30]. 0.02 g of modified silica pellet is prepared with a diameter of 13 mm at 0.7 kPa using die set for compaction. The pellet is placed in a sample cell, and the system is evacuated for 4 h at 160 °C. The sample chamber is cooled to room temperature and the IR spectrum is obtained. Subsequently, water vapor is introduced into the sample chamber until the relative pressure is about 0.1. After adsorption reached equilibrium, the FT-IR spectrum is recorded. These steps are repeated with increasing vapor pressure until the maximum relative pressure is reached. The amount of water vapor (S_{OH}) is calculated from the areas of the silanol peaks as follows:

$$S_{OH} = \frac{S_A - S_{CH}}{I(1864 \text{ cm}^{-1}) - I(2450 \text{ cm}^{-1})} \quad (2)$$

where S_A is the area of the peaks in the 2450–4000 cm^{-1} region, S_{CH} is the area of the peaks in the 2750–3000 cm^{-1} region which indicated the C–H stretching region, and $I(1864 \text{ cm}^{-1})$ and $I(2450 \text{ cm}^{-1})$ are the absorbance at the respective wavelengths.

3-2-5 Preference dispersion test

The macroscopic wettability of the modified silica samples is determined by a preference dispersion test. Fumed silica sample is dried at 160 °C for 4 h. The sample is then stirred in distilled water, and the wettability is determined by visual observation. It is noted that hydrophilic samples are

dispersed in the water, while hydrophobic samples are floated on the water surface. The samples are slowly placed in a thermostatic tank at 30 °C, and observed for 6 h with an additional dispersion every 30 minutes [15, 30].

3-3. Results and Discussion

3-3-1 Characteristics of modified fumed silica surface

The degree of surface modification ratio, θ %, as a function of alcohol content is shown in Fig. 3-1. Here, the modification ratio is the fraction of modified hydroxyl groups, relative to the total hydroxyl groups on the surface of unmodified silica. It is shown that the modification ratio increases more drastically for *n*-modified silica when the butyl alcohol content increases, as compared to *t*-modified silica. The modification ratios of *n*- and *t*-silica are 30 % and 20 % when 0.1 ml/g of *n*- and *t*-butyl alcohol are used, respectively. As the alcohol concentration increases to >0.1 ml/g, the modification ratio increases at a slower rate than that at lower concentrations. The decrease in modification rate at butyl alcohol concentrations higher than 0.1 ml/g is because of the steric hindrance of the modification agents that are already present on the surface of the silica particles. The highest modification ratios obtained for *n*-silica and *t*-silica are 49 % and 39 % when 0.5 ml and 1.5 ml of alcohol were added, respectively.

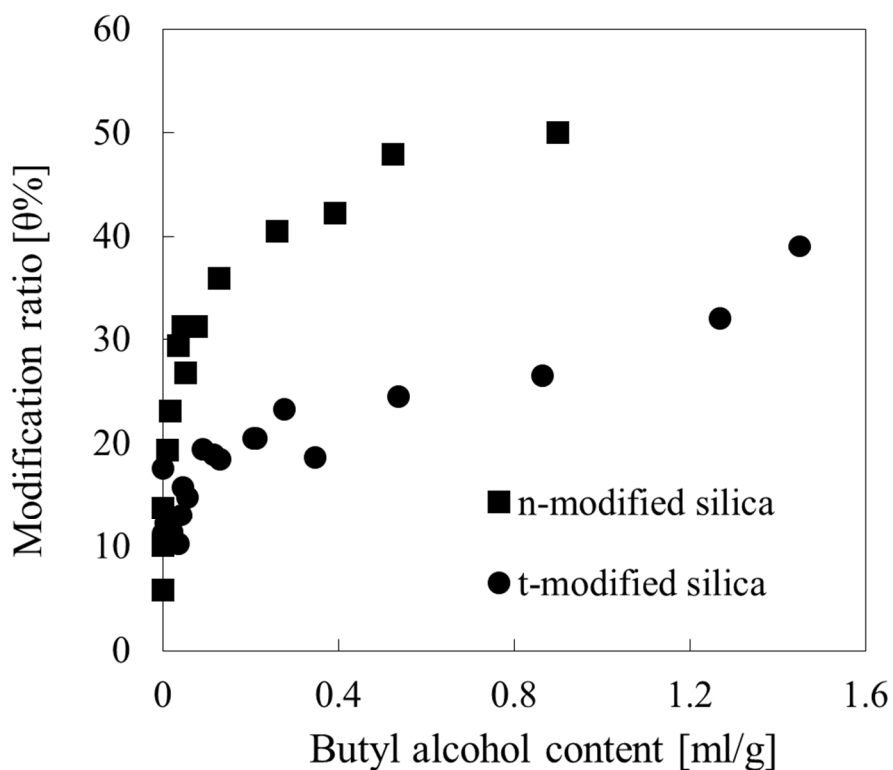


Fig.3-1 Change in modification ratio of *n*-silica and *t*-silica as a function of amount butyl alcohol contents.

The surface modification by butyl alcohols proceeds via a dehydration reaction of the hydroxyl groups on the silica surface and the R–OH groups in the alcohol. As a result, Si–OH is replaced by Si–O–R, where R is either *n*- or *t*-butoxy groups. The differences in the modification ratios of *n*- and *t*-modified silica are attributed to the chemical structure of the butyl alcohols. The *n*-butoxy group is relatively narrow and has flexible conformation, while the *t*-butoxy group is very bulky and has rigid conformation. Therefore, the difference between the nature of chains in *n*-butoxy and *t*-butoxy isomers is the main reason for the difference in modification ratio. The effect of structural differences is

confirmed by calculating the area that each butoxy group occupies on the silica surface [31, 32]. The results are summarized in Table 3-1.

Table 3-1. Occupancy areas of *t*- and *n*-butoxy groups on silica surface. σ_1 , is calculated from Van der Waals radii and Bond lengths; σ_2 is calculated based on the surface coverage of hydroxyl groups on silica surface at *n*-butoxy = 49 % and *t*-butoxy = 39 %. σ_3 is calculated from surface coverage at turning point of *n*-butoxy and *t*-butoxy occur when modification ratio is 30 % and 20 %, respectively.

Occupancy area	<i>n</i> -butoxy groups	<i>t</i> -butoxy groups
	[nm ²]	[nm ²]
σ_1	0.3–1.7	0.6
σ_2	0.7	0.9
σ_3	1.2	1.4

The theoretical occupancy area of each butoxy group, σ_1 , is calculated from the van der Waals radii and bond lengths. σ_2 is the occupancy area of each type of butoxy group, which is calculated from the TG-DTA results by assuming 100 % surface coverage of hydroxyl groups on the silica surface at the maximum modification ratios (*n*-butoxy = 49 % and *t*-butoxy = 39 %). σ_3 is the occupancy area of each type of butoxy group calculated from TG-DTA results assuming 100 % surface coverage at the turning points of the modification ratios (turning point of *n*-butoxy and *t*-butoxy occur when

modification ratio is 30 % and 20 %, respectively). The σ_1 value of the *n*-butoxy groups varies in a range instead of a specific value because of conformational changes. The lower limit ($\sigma_1 = 0.3 \text{ nm}^2$) indicates that the *n*-butoxy groups are well oriented vertically on the silica surface, and the upper limit (1.7 nm^2) corresponds to the *n*-butoxy chains lying parallel to the silica surface. At the maximum modification ratio, the occupancy area for *n*-modified silica is calculated as $\sigma_2 = 0.7 \text{ nm}^2$, while the theoretical minimum occupancy area of *n*-butoxy group (σ_1) is 0.3 nm^2 . At the turning point, the calculated occupancy area of *n*-modified silica is 1.2 nm^2 , which is smaller than the theoretical maximum, 1.7 nm^2 . In contrast, the experimentally determined occupancy area for the *t*-butoxy group ($\sigma_2 = 0.9 \text{ nm}^2$) is larger than the theoretical value at the turning point, $\sigma_1 = 0.6 \text{ nm}^2$.

When the density of *n*-butoxy modifiers on the surface of silica is high, *n*-butoxy chains tend to be oriented perpendicular to the silica surface, which reduces the average occupancy area close to the theoretical minimum, 0.3 nm^2 . In case of lower densities, *n*-butoxy chains will lay parallel to the surface of silica occupying an area close to the theoretical area, 1.7 nm^2 . At the maximum modification ratio of *n*-modified silica with modification ratio of 49 %, the average occupancy area of the *n*-butoxy groups is estimated to be 0.3 nm^2 . This is not plausible because this theoretical value does not include steric hindrance. The occupancy area of 1.2 nm^2 calculated at the turning point of *n*-modified silica with modification ratio of 30 %, is more reasonable, as there is not enough space for all chains to lay parallel to the silica surface. Based on these results, the *n*-butoxy groups experience significant steric

hindrance at the modification ratio of 30 %, above which the *n*-butoxy groups begin to be oriented perpendicular to the silica surface.

In addition to silanol groups, the unmodified silica surfaces contain siloxane groups [1]. Hence, some sites are inaccessible to the *t*-butoxy groups. Since the *t*-butoxy groups are significantly more bulky and less flexible than the *n*-butyl chains, they experience greater steric hindrance; thus, $\sigma_2 = 0.9 \text{ nm}^2$ is a reasonable occupancy area for the *t*-butoxy groups.

Fig. 3-2 shows the FT-IR spectrum of each type of hydroxyl group on the silica surface. There are two types of hydroxyl groups on the surface of fumed silica particles: (1) free hydroxyl groups and (2) H-bonded hydroxyl groups [33]. Free hydroxyl groups can exist as isolated and geminal groups. Moreover, H-bonded hydroxyl groups possess terminal H bonded and non-terminal H bonded hydroxyl groups. The spectral peak of the free hydroxyl groups occurs at 3747 cm^{-1} , H-bonded hydroxyl groups at $3740\text{--}3000 \text{ cm}^{-1}$, and terminal H-bonded hydroxyl groups at either 3720 or 3725 cm^{-1} [34,35]. The vibration band for the butoxy group on the modified silica surface occurs at $3000\text{--}2800 \text{ cm}^{-1}$ because of C–H stretching. Since the H-bonded hydroxyl groups are at a short distance from their neighboring hydroxyl groups, the H-bond interactions of the terminal hydroxyl groups are weak, and therefore, their IR peaks are shifted to either 3720 or 3725 cm^{-1} [33] .

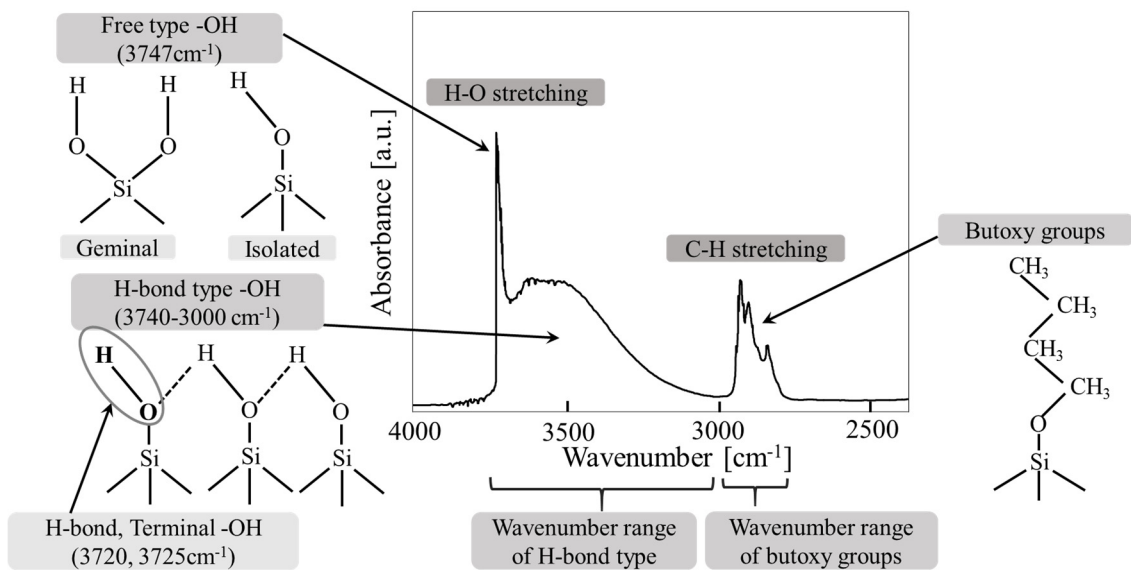


Fig.3-2 FT-IR spectrum of each type of hydroxyl group on silica surface.

Fig. 3-3 shows the FT-IR spectra of *n*- and *t*-modified silica at various modification ratios. The peak area of the free hydroxyl groups at 3747 cm^{-1} decreases significantly with increasing modification ratio, and almost disappeared at the maximum modification ratios (49 % of *n*-silica and 39 % of *t*-silica). The peaks at $2800\text{--}3000\text{ cm}^{-1}$, ascribed to the alkyl chains, increase with increasing modification ratio. A similar trend is confirmed for both *n*- and *t*-modified silica particles; the increasing modification ratios are in good agreement with the results shown in Fig. 3-1.

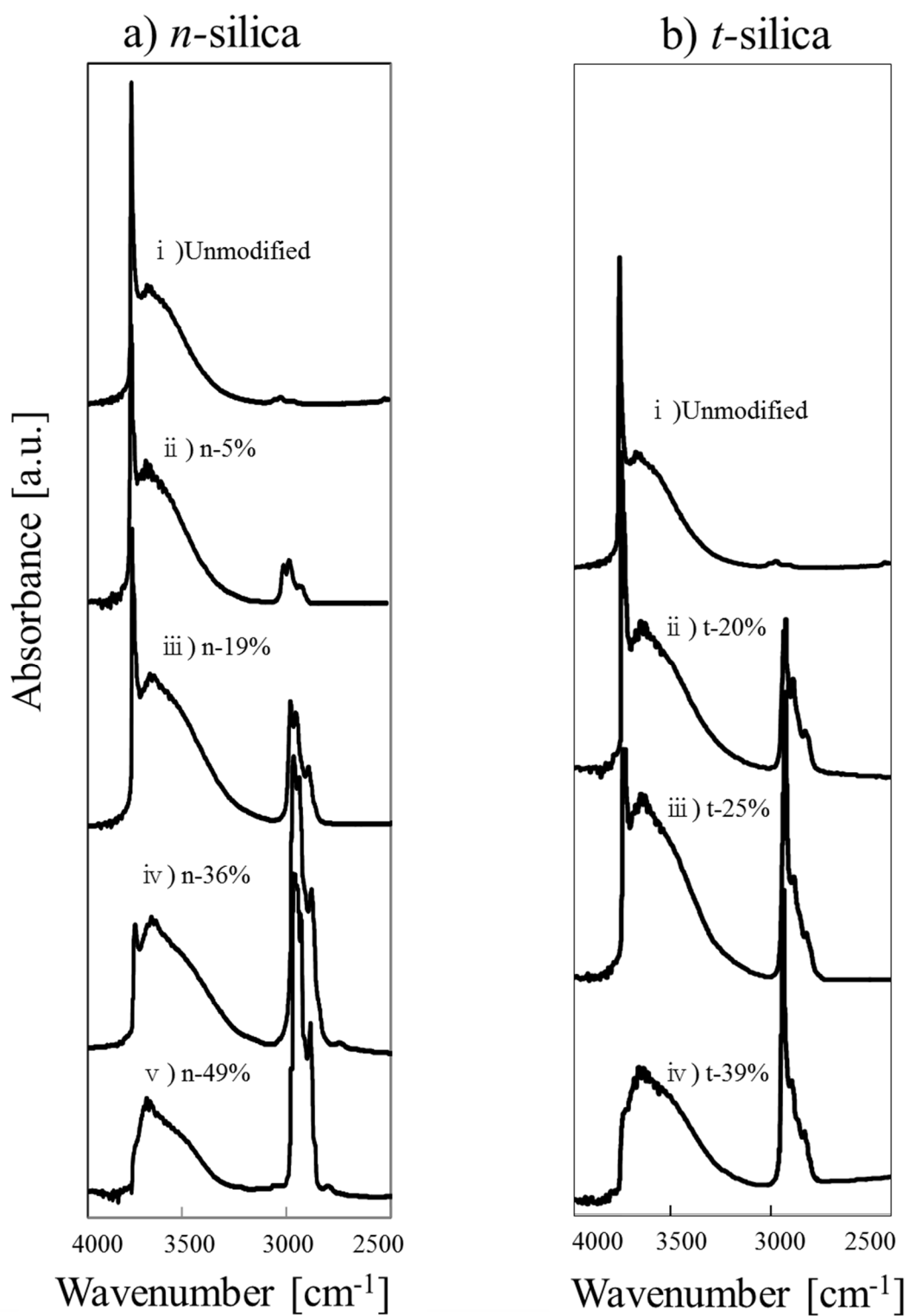


Fig. 3-3 FT-IR spectra of various modification ratio of *n*- and *t*-silica.

3-3-2 Macroscopic wettability evaluated by preference dispersion test

Preference dispersion test results which observed after 3h are shown in Fig. 3-4, and the photograph of the example samples shows Fig. 3-5. The *n*-modified silica samples with a modification ratio of < 30 % are well dispersed in water, indicating their hydrophilicity. The *n*-modified silica samples with the modification ratio of 30–32 % are partially hydrophobic, and samples with modification ratio of > 32 % are completely hydrophobic. In contrast, the *t*-modified silica sample is hydrophilic when the modification ratio is < 25 %, partially hydrophobic when the modification ratio is 25%–26.5 %, and completely hydrophobic when the modification ratio is > 26.5 %. A comparison between Fig. 3-1 and Fig. 3-4 shows that the modification ratio and hydrophilic/hydrophobic turning points differ for *t*-modified silica, while they are consistent for *n*-modified silica.

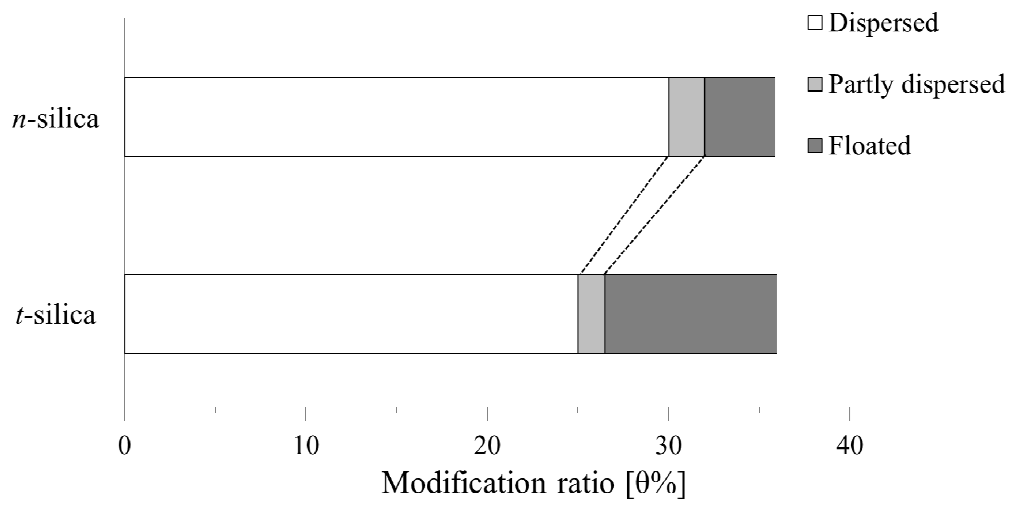


Fig. 3-4 Results of the preference dispersion test for *n*-silica and *t*-silica observed after

3h.

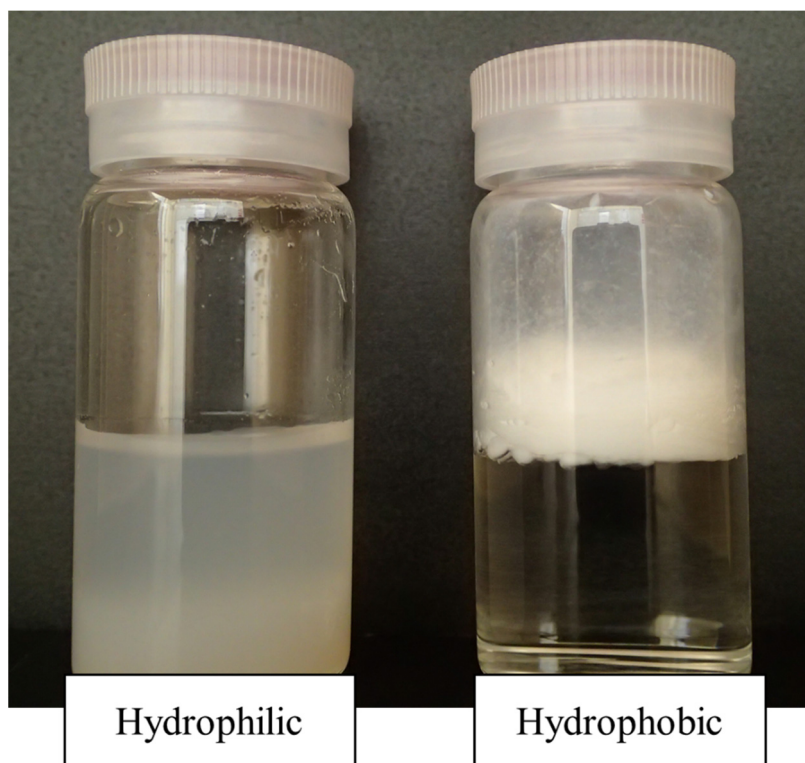


Fig. 3-5 Photograph of the hydrophilic and hydrophobic samples of preference

dispersion test.

It is noted that *n*-modified silica with modification ratios of 30 % and 32 % are initially partially hydrophobic; however, they become hydrophilic after being dispersed in water for 6 h. This indicates that the surface of *n*-modified silica with the modification ratio of 30–32% is hydrolyzed in water due to the accessibility of the Si-O-*n*Bu linkage because of the flexibility of the *n*-butyl chains. In contrast, the bulky *t*-butoxy groups remain stable even after 6 h because the Si-O-*t*Bu linkage is inaccessible by the surrounding water molecules.

3-3-3 Amount of water vapor adsorption on unmodified silica observed by FT-IR

The water vapor adsorption isotherm and FT-IR spectra of unmodified silica under different relative vapor pressures are shown in Fig. 3-6. As shown in Fig. 3-6 a), at $P/P_0 = 0.7$ a single water molecule is adsorbed onto each surface hydroxyl group [33]. At $P/P_0 = 0.8$, two water molecules are adsorbed on each hydroxyl group [33], suggesting that the surface hydroxyl groups are saturated with water molecules. However, free hydroxyl groups are still present on the surface of silica at $P/P_0 = 0.8$. The free hydroxyl peak at 3747 cm^{-1} decreases with increasing relative pressure and a slight shift to a lower wavenumber is observed at 3720 and 3725 cm^{-1} , as shown in Fig. 3-6 b). These results demonstrate that water molecules are not uniformly adsorbed on the silica surface. Instead, they are partially adsorbed onto the H-bonded hydroxyl groups and formed a two-dimensional layer on the

silica surface, as schematically illustrated in Fig. 3-7.

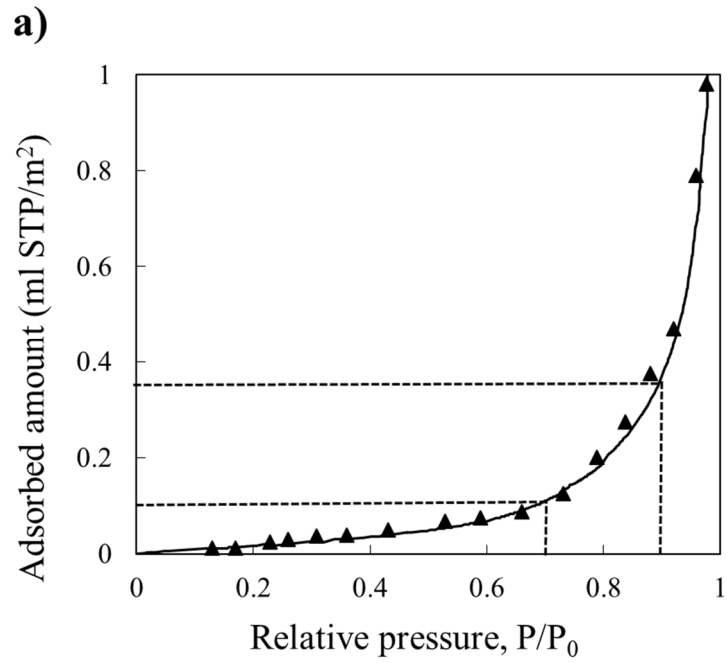


Fig. 3-6 a) The water vapor adsorption isotherm

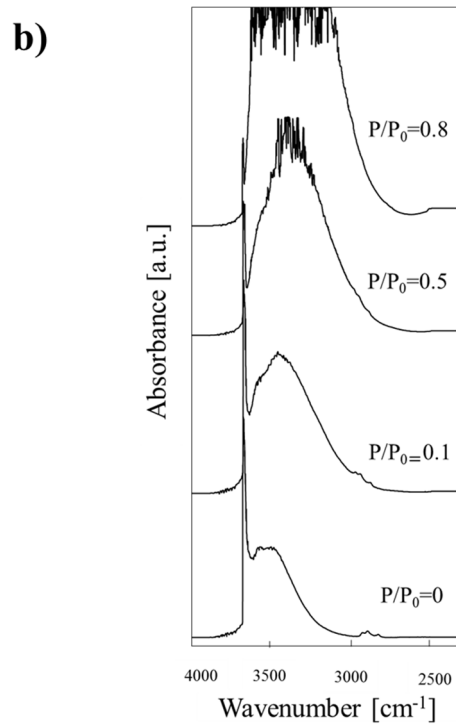


Fig. 3-6 b) FT-IR spectra of unmodified silica under different relative vapor pressures.

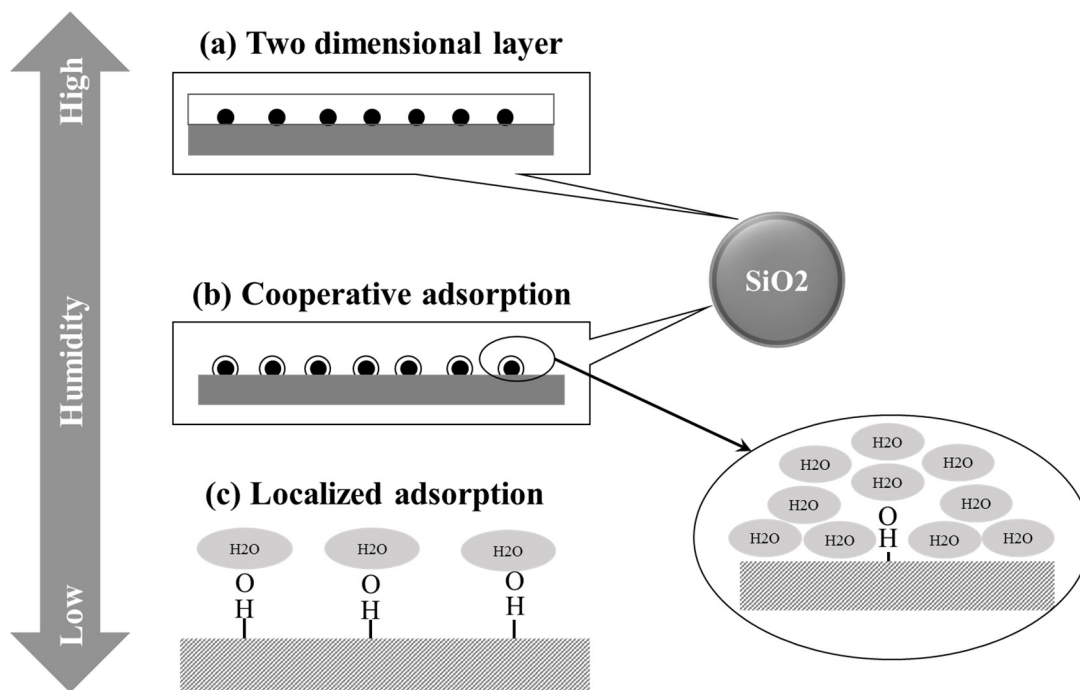


Fig. 3-7 Adsorption mechanisms of water on silica particle surface.

The water adsorption mechanisms on silica surfaces have been reported by Fuji and Takahashi [37]. The adsorption mechanism at low and humidities are shown in Fig. 3-7. As shown in Fig. 3-7 (a), at low humidity water molecules undergo localized adsorption. As humidity increases, more water molecules are adsorbed in a cooperative process, Fig. 3-7(b). At a high humidity water molecules from the two-dimensional layer, Fig. 3-7(c), resulting in greater water adsorption. The continuous formation of a two-dimensional water layer followed by additional water adsorption resulted in the formation of multiple layers of water molecules on the surface of silica particles. The amount of water adsorption increases rapidly with high relative pressure. Finally, the formation of a continuous two-dimensional layer of water molecules affects the wettability of the silica surface.

This water adsorption mechanisms has not been revealed by microscopic observation. Based on the Fig. 3-6, the formation of the two-dimensional layer and a continuous two-dimensional layer of water molecules were revealed by water vapor adsorption test on silica surface microscopically.

3-3-4 Microscopic wettability evaluated by the amount of water vapor adsorption by FT-IR

3-3-4 (1) Observation of water adsorption behavior on modified silica surface

The observed water adsorption behavior of modified silica surfaces is explained based on the adsorption mechanisms of unmodified silica surfaces [36] as explained in the following. Based on the results of preference dispersion, *n*-modified silica with modification ratio of 19 % and *t*-modified silica with modification ratio of 20 % are chosen as representative hydrophilic samples. In addition, *n*-modified silica with modification ratio of 49 % and *t*-modified silica with modification ratio of 39 % are chosen as representative hydrophobic samples. The water vapor adsorption of these modified silica particles is examined by FT-IR.

Fig. 3-8 shows the FT-IR spectra of hydrophilic *n*-modified silica with modification ratio of 19 % and *t*-modified silica with modification ratio of 20 % at different relative vapor pressures. In these modified silicas, the peak intensity of free hydroxyl group at 3747 cm^{-1} decreases with increasing the relative pressure. However, the rate of peak area decrease is slower than that of the unmodified silica.

In addition, similar peak shifts to lower wavenumber are observed in the 3740–3680 cm^{-1} plateau.

The decrease in free hydroxyl groups is more significant for the *t*-modified silica with modification ratio of 20 % sample than that of *n*-modified silica with modification ratio of 19 % sample because: On one hand, *n*-butoxy groups lie flat on the silica surface, corresponding to ~ 0.5 butoxy groups/ nm^2 , and shielding free hydroxyl groups from water molecules [15]. On the other hand, *t*-butoxy groups are conformationally stable. Therefore, some of the remaining hydroxyl groups are protected from modification by steric hindrance of *t*-butoxy groups. The presence of the butoxy groups hinders the formation of a continuous two-dimensional water layer, resulting in smaller peak reductions (3747 cm^{-1}) and slighter shift (3740–3680 cm^{-1}) compared to those of unmodified silica.

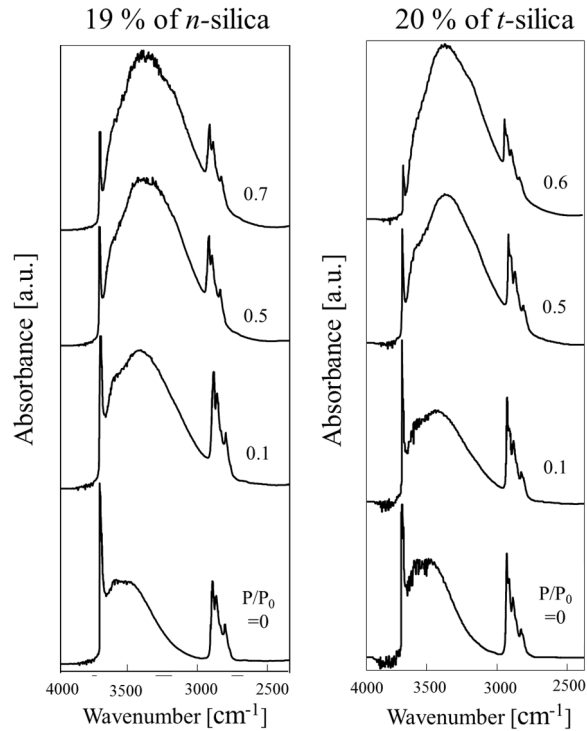


Fig. 3-8 FT-IR spectra of modified silica at each relative pressure during the water vapor process obtained from modification rate of 19 % of *n*-silica and 20 % of *t*-silica.

Fig. 3-9 shows the FT-IR spectra of the hydrophobic 49 % *n*-modified silica samples and 39 % *t*-modified silica samples at different relative vapor pressures. In these samples, all of the free hydroxyl groups are modified, and therefore do not appear in the FT-IR spectra. The two samples exhibit similar trends during water adsorption. The peak area of H-bonded hydroxyl group at 3740–3000 cm^{-1} increases with increasing relative pressure. Although the surfaces of these samples are hydrophobic, the proportion of H-bonded hydroxyl groups increases because water molecules preferentially adsorb on these hydroxyl groups, resulting in the formation of a two-dimensional layer of water on the surface

of silica particles. This result is in good agreement with those of unmodified and hydrophilic modified silica particles. Therefore, water molecules can adsorb onto H-bonded hydroxyl groups regardless of the surface condition, although the accessibility of these hydroxyl groups is affected by surface modifications.

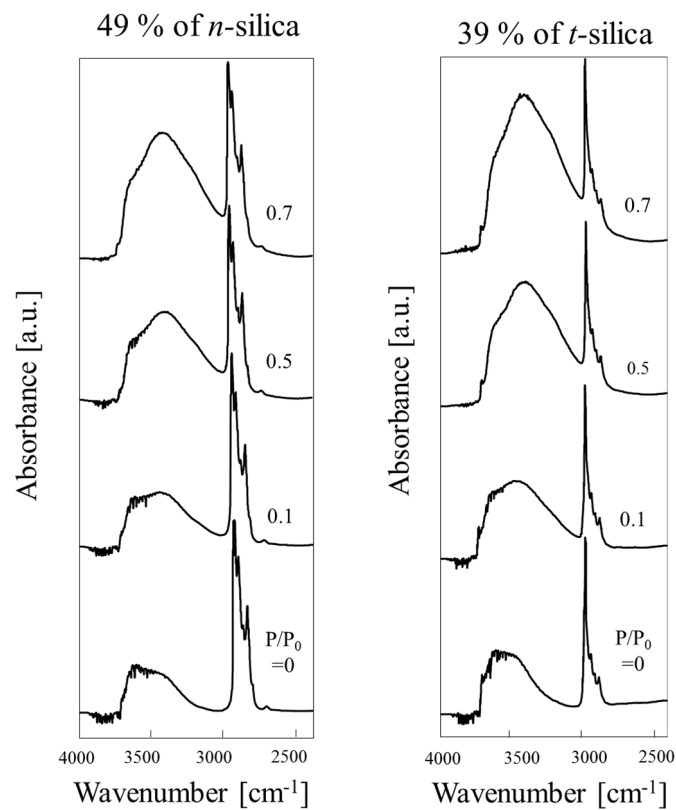


Fig. 3-9 FT-IR spectra of modified silica at each relative pressure during the water vapor process obtained from modification rate of 49 % of *n*-silica and 39 % of *t*-silica.

3-3-4 (2) Calculation of the amount of adsorbed hydroxyl groups from peak area of FT-IR

Water vapor adsorption is estimated from the peak area of the hydroxyl group. The relationship between the relative pressure and the O–H stretching peak area of H-bonded hydroxyl groups (4000–2450 cm^{-1} , S_{OH}) for *n*- and *t*-modified silica samples are shown in Fig. 3-10 a) and 3-10 b), respectively. S_{OH} is calculated by equation (2). Although the absorption peak of the free hydroxyl groups (3747 cm^{-1}) is included within this spectral range, it can be ignored since its contribution is negligible compared to that of H-bonded hydroxyl groups. As shown in Fig. 3-10 a), the 19 % *n*-modified silica sample exhibits a similar trend to that of unmodified silica shown in Fig. 3-10 b), although the peak area in the spectrum of the former is smaller throughout the range of the relative pressure test. The trends in the 32 % and 36 % *n*-modified silica are similar for $P/P_0 \leq 0.5$, and changes are more sluggish than those of 19 % *n*-modified silica are. In the case of the 32 % *n*-modified silica, a significant increase in peak area is observed at $P/P_0 \geq 0.5$. The peak area for the 36 % *n*-modified silica increases more linearly upon increasing the relative pressure.

As shown in Fig. 3-10 b), the unmodified silica shows the largest peak area of the samples and its hydroxyl group peak area gradually increases with increasing relative pressure. The 20 % and 39 % *t*-modified silica samples show similar trends and almost identical peak areas at $P/P_0 \leq 0.5$. The 20 % *t*-modified silica is hydrophilic, while the 39 % *t*-modified silica sample is hydrophobic as confirmed by a preference dispersion test. For 20 % *t*-modified silica, a significant increase in adsorption is observed at $P/P_0 \geq 0.5$, attributed to the shielding of free hydroxyl groups by *n*-butyl chains on the

surface of 19 % *n*-modified silica.

At high relative pressures, water molecules are more strongly adsorbed on the H-bonded hydroxyl groups than on the free hydroxyl groups. Therefore, the hydroxyl group peak area of unmodified silica gradually increases. In contrast, only a small fraction of free hydroxyl groups remains on 39 % *t*-modified silica because of its hydrophobicity. However, the water vapor adsorption of the H-bonded hydroxyl groups on the 39 % *t*-modified silica gradually increases. Although the surface of the *t*-modified silica with modification ratio of 20 % is hydrophilic, water molecules are preferentially adsorbed on the H-bonded hydroxyl groups at low relative pressures. This proves that the initial water adsorption process at low relative pressure is similar for both *n*- and *t*-modified silica surfaces.

As already shown in Fig. 3-1, the steric hindrance effect of the *t*-butyl groups are evident in the 20 % *t*-modified silica sample. At this modification ratio, a large amount of *t*-butoxy groups are supposed to be present on the surface of silica. However, its surface remains hydrophilic because of the presence of free hydroxyl groups. That is why a rapid increase in water adsorption is observed for this sample at $P/P_0 \geq 0.5$. In contrast, the 39 % *t*-modified silica is hydrophobic and only a small amount of free hydroxyl groups are expected to exist on its surface. Hence, the rapid increase in adsorption at $P/P_0 \geq 0.5$ is not observed in the 39 % *t*-modified silica.

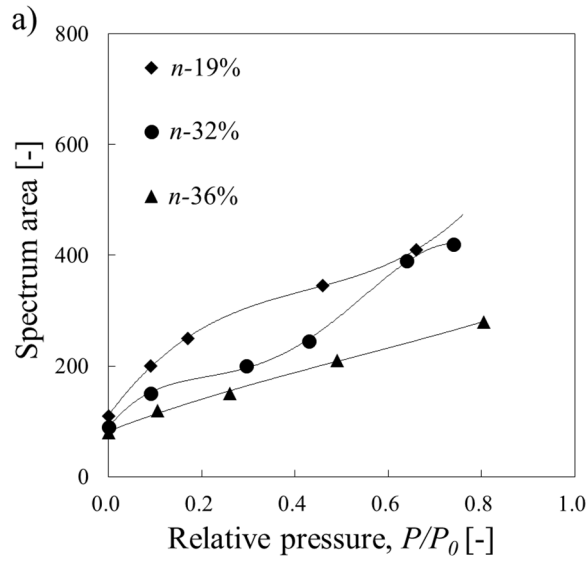


Fig. 3-10 a) Relationships between relative pressure and spectrum area of -OH stretching for modification rate of 19 %, 32 %, and 36 % of *n*-silica.

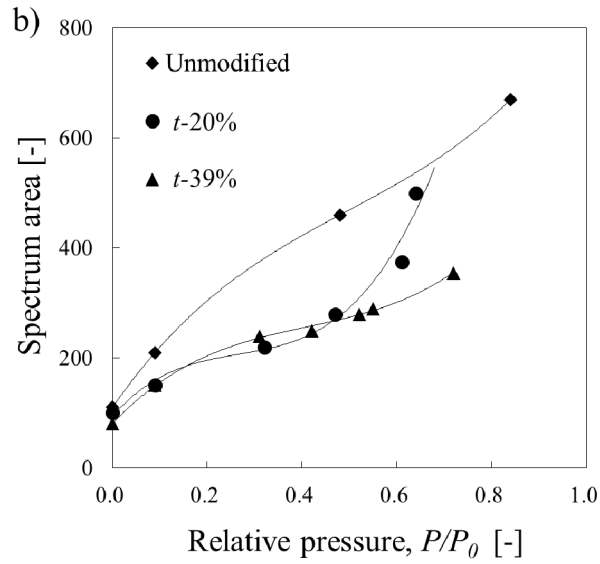


Fig. 3-10 b) Relationships between relative pressure and spectrum area of -OH stretching for modification rate of 20 %, and 39 % of *t*-silica, and unmodified silica.

3-4. Conclusions

Fumed silica surfaces were modified with either *n*- or *t*-butyl alcohols at various concentrations. Changes in surface wettability were observed macroscopically by water preference dispersion tests and microscopically by the water vapor adsorption test determined by FT-IR. The bulky structure and unchanged conformation was found to be more effective for a hydrophobic surface and was confirmed by the macroscopic method. The same amount of butyl alcohols with different molecular structures have different hydrophobic effects.

1. Macroscopic water preference dispersion test confirmed that butyl alcohols with different molecular structures effectively modified the surface of silica particles with different hydrophobicity. Silica modified by bulky, rigid, *t*-butoxy groups was more hydrophobic than *n*-butyl-modified silica was.
2. Microscopic water vapor adsorption test by FT-IR confirmed that water molecules preferentially adsorbed onto H-bonded hydroxyl groups during the initial stage of adsorption. Therefore, the hydrophobic effects of different structural surfaces became more distinct at $P/P_0 \geq 0.5$.
3. The hydrophilic/hydrophobic turning points of the *n*- and *t*-silica were in accordance with the observation results by the preference dispersion test and by the water vapor adsorption test.

Furthermore, macroscopic and microscopic observation results were correlated.

References

- [1] Evonik. AEROSIL® - fumed silica Technical overview. Available at <https://www.aerosil.com/sites/lists/RE/DocumentsSI/Technical-Overview-AEROSIL-Fumed-Silica-EN.pdf>. (accessed on April 1st, 2017).
- [2] F. Sadeghi, F. Mosaffa, H. A. Garekani, Effect of Particle Size, Compaction Force and Presence of Aerosil 200 on the Properties of Matrices Prepared from Physical Mixture of Propranolol Hydrochloride and Eudragit RS or RL, *Iranian Journal of Basic Medical Sciences*, 10 (2007) 197–205.
- [3] A. Jaroenworat, N. Pijarna, N. Kosachana, R. Stevens, Nanocomposite TiO₂–SiO₂ gel for UV absorption, *Chem. Eng. J.*, 181–182 (2012) 45–55.
- [4] M. C. Pohl, D. A. Griffiths, The Importance of Particle Size to the Performance of Abrasive Particles in the CMP Process, *J. Electron. Mater.*, 25 (1996) 1612–1616.
- [5] Y. Kang, Y.N. Prasad, I. Kim, S. Jung, J. Park , Synthesis of Fe metal precipitated colloidal silica and its application to W chemical mechanical polishing (CMP) slurry, *J. Colloid Interface Sci.*, 349 (2010) 402–407.
- [6] The Additives for the Coating Material, *Journal of the Japan Society of Color Material*, 83 (2010) 430–439.
- [7] B. Jaúregui-Beloqui, J.C. Fernández-García, A.C. Orgilés-Barceló, M.M. Mahiques-Bujanda, J.M. Martín-Martínez , Rheological properties of thermoplastic polyurethane adhesive solutions containing

fumed silicas of different surface areas, *Int. J. Adhesion & Adhesives*, 19 (1999) 321–328.

[8] T. Mizutani, K. Arai, M. Miyamoto, Y. Kimura, Application of silica-containing nano-composite emulsion to wall paint: A new environmentally safe paint of high performance, *Prog. Org. Coat.*, 55 (2006) 276–283.

[9] An e-book to Johokiko CO.,LTD. Available at <http://www.johokiko.co.jp>, (accessed on April 1st, 2017).

[10] I. Stevenson, L. David, C. Gauthier, L. Arambourg, J. Davenas, G. Vigier, Influence of SiO₂ fillers on the irradiation ageing of silicone rubbers, *Polymer*, 42 (2001) 9287–9292.

[11] A. Kawamura, C. Takai, M. Fuji, T. Shirai, Effects of Water Adsorption on Dispersibility of Fumed Silica in Mixed Organic Solvents of Ethanol and Hexane, *J. Soc. Powder Technol., Jpn.*, 48 (2011) 755–760.

[12] H. Kamiya and M. Iijima, Dispersion behavior control of nanoparticles and its applications, *The Micromeritics*, 55 (2012) 12–18.

[13] Surface interactions of dimethylsiloxy group-modified fumed silica, H. Barthel, *Colloids Surf., A*, 101 (1995) 217-226.

[14] A. Kawamura, H. Liu, C. Takai, T. Takei, H. K. Razavi, M. Fuji, Surface modification of fumed silica by photo-dimerization reaction of cinnamyl alcohol and cinnamoyl chloride, *Adv. Powder Technol.*, 27 (2016) 765–772.

- [15] M. Fuji, S. Ueno, T. Takei, T. Watanabe, M. Chikazawa, Surface structural analysis of fine silica powder modified with butyl alcohol, *Colloid. Polym. Sci.*, 278 (2000) 30–36.
- [16] A. Kawamura, C. Takai, M. Fuji, T. Shirai, Effect of solvent polarity and adsorbed water on reaction between hexyltriethoxysilane and fumed silica, *Colloids Surf., A*, 492 (2016) 249–254.
- [17] M. Sasaki, H. Honda, S. Nakano, S. Fuji, Y. Nakamura, K. Nagata, Structure of silica-treated layer on silica particle surface analysis using pulse NMR, *J. Adhes. Soc. Jpn.*, 45 (2009) 88–93.
- [18] A. Krysztafkiewicz, B. Rager, NIR studies of the surface modification in silica fillers, *Colloid. Polym. Sci.*, 266 (1988) 485–493.
- [19] M. Aoki, Y. Chikashige, T. Komatsubara, M. Ueda, *Surface Structure of Fumed Silica*, The Imaging Society, Japan, 54 (2015) 140–147.
- [20] H. Barthel, Surface interactions of dimethylsiloxy group-modified fumed silica, *Colloids Surf., A*, 101 (1995) 217–226.
- [21] S.J. Klatt, T.L. Beck, Molecular dynamics of tethered alkanes: Temperature-dependent behavior in a high-density, *J. Phys. Chem.*, 97 (1993) 5727–5734.
- [22] Y. Zhan, X. Li, W.L. Mattice, Simulations of self-assembled monolayers with the same surface density but different grafting patterns, *Langmuir*, 11 (1995) 2103–2108.
- [23] U. Essmann, L. Perera, M.L. Berkowitz, The origin of the hydration interaction of lipid bilayers from MD simulation of dipalmitoylphosphatidylcholine membranes in gel and liquid crystalline

phases, *Langmuir*, 11 (1995) 4519–4531.

[24] S.W. Myung, M.S. Kim, C.N. Yoon, J.S. Park, W.S. Ahn, Gas chromatographic-electron-impact chemical ionization mass spectrometric identification of cinmetacin and its metabolites in human urine, *J. Chromatogr.*, 660 (1994) 75–84.

[25] S. Brunauer, P. H. Emmett, E. Teller, Adsorption of gases in multimolecular layers, *J. Amer. Chem. Soc.*, 60 (1938) 309–319.

[26] K. R. Lange, Reactive organic molecules on silica surfaces, *Chem. Ind.*, 36 (1969) 1273–1274.

[27] H. Utsugi, H. Horikoshi, T. Matuszawa, Mechanism of esterification of alcohols with surface silanols and hydrolysis of surface esters on silica gels, *J. Colloid. Interface. Sci.*, 50 (1975) 154–161.

[28] M. Fuji, C. Takai, Y. Tarutani, T. Takai, M. Takahashi, Surface properties of nanosize hollow silica particles on the molecular level, *Adv. Powder Technol.*, 18 (2007) 81–91.

[29] M. Fuji, M. Chikazawa, Reactivity to water and alcohol of siloxane formed by heat-treatment on silica powder surface, *J. Soc. Powder Technol. Jpn.*, 37 (2000) 19–25.

[30] M. Fuji, H. Iwata, T. Takei, T. Watanabe, M. Chikazawa, The change in the water vapor affinity of fine particle loaded with trimethylsilyl groups, *J. Soc. Powder Technol. Jpn.*, 32 (1995) 649–654.

[31] A. L. McClellan, H. F. Harnsberger, Cross-sectional areas of molecules adsorbed on solid surfaces, *J. Colloid. Interface. Sci.*, 23 (1967) 577–599.

[32] K. Kaneko, Fractal and solid surface analysis, *Chemistry (Jpn.)*, 45 (1990) 525–528.

- [33] M. Fuji, M. Chikazawa, The influence of the surface conditions on the adhesion force between particles, *J. Jpn. Soc. Color Mater.*, 73 (2000) 444–451.
- [34] A. Zecchina, S. Bordiga, G. Spoto, L. Marcobese, G. Petrid, G. Leofanti, M. Padovan, Silicallte characterization. 2. IR spectroscopy of the interaction of CO with internal and external hydroxyl group, *J. Phys. Chem.*, 96, 4991–4997 (1992).
- [35] B.C. Bunker, D.M. Haaland, K.J. Ward, T.A. Michalske, W.L. Smith, J.S. Binkley, C.F. Melius, C.A. Balfe, Infrared spectra of edge-shared silicate tetrahedral, *Surf. Sci.*, 210 (1989) 406–428.
- [36] M. fuji, M. Takahashi, Surface Properties of Particle and Adhesion Force between Particles, Annual Report of the Advanced Ceramics Research Center, Nagoya Institute of Technology, 12 (2002) 9–16.

Chapter 4: Surface modification of fumed silica by photo-dimerization reaction of cinnamyl alcohol and cinnamoyl chloride

4-1. Introduction

In recent years, three dimensional (3D) printers have started being used in various fields [1–3]. 3D printers can create structures by reading out the three-dimensional data generated by Computer Aided Design (CAD) [4, 5]. The start of that technology was the acquisition of a patent on 3D stereo lithography [6, 7] by Chuck Hull who was an American engineer in 1987. His first working 3D printer was created in 1984. He published a number of patents on the concept of 3D printing, many of which are used in today's additive manufacturing processes. [8–10]. In addition, due to the invention of various molding method technologies, Fused Deposition Modeling [11-13], Inkjets, [14–17] and Selective Laser Sintering [18–22] are also carried out using the 3D printer [23]. Following the evolution of the technology and cost reductions, the 3D printer market is rapidly growing. Along with this development, the demand for resins for use in each manufacturing method has been rapidly rising with advances in the technology. At present, an ultraviolet (UV) curing resin with an acrylic resin base and a thermoplastic resin with an acrylonitrile-butadiene-styrene resin base are primarily used in the 3D printer material. With the inkjet printer becoming popular due to reduction in size, the market share growth of UV curing resin is significantly expanding on a global scale [24]. The use of UV curing resins has attracted attention in recent years from the viewpoint of a reduced environmental burden because it reduces the emission of volatile organic compounds (VOCs) due to instant formation of the

coating film by UV irradiation [25]. A remarkable feature of the UV resin is that it does not need a drying process for removing the solvent, thus leading to shortened working duration.

In the past decade, nanosilica particles have been widely introduced into polymers to provide functionalities that have never existed before [26]. There are some reports that the nanosilica contained in UV cured resin provided new functions for the polymers. Nanosilica particles are used as a filler in UV acrylate paints where they crosslink and cure the silica and UV curing resin upon UV irradiation [27]. However, since the amount of silica powder to be added to a UV resin is limited, it is difficult to obtain a UV resin containing a large amount of the inorganic material. If the amount of inorganic material included is greater than the amount of organic polymer is, the 3D printing process may possibly be more environmentally friendly. Additionally, one of the optical shaping methods requires an additional step for excessive resin removal. Thus, it can reduce the surplus resin and increase efficiency due to a shorter processing time. If the inorganic material can function by itself upon photo-irradiation, its content rate and function in the polymer can be improved.

There are two kinds of photo-dimerization functional groups: cinnamoyl based and cinnamylidene based groups. Many compounds functionalized with these groups, such as activated ethylene and polycyclic compounds, can undergo photo-dimerization involving the intermolecular cross-linking bonds in the polymer. As cinnamoyl groups develop the [2+2] cyclization by the photo-dimerization reaction, polyvinyl cinnamate, which was made by the esterification reaction of the

cinnamoyl groups and PVA, becomes insoluble depending on the photo-crosslinking [28]. Therefore, polyvinyl cinnamate applied as a negative photoresist is a representative example of the photo-sensitive resin. Taking inspiration by the photo-reaction of polyvinyl cinnamate, photo-functional groups might be introduced on the surface of the fumed silica thus creating functional particles capable of photo-crosslinking by optical irradiation. In addition, nano-sized inorganic functional materials, which are difficult to be obtained by modern technology, can be developed [29, 30].

Herein, it was shown that the cinnamoyl chloride has a cinnamyl group ($C_6H_5-CH=CH-CH_2-$) and cinnamyl alcohol has cinnamoyl group ($C_6H_5-CH=CH-CHO-$) on the fumed silica surface because their terminals substituted by $-Cl$ and $-OH$ have a high reactivity with the silanol groups. Furthermore, it was determined that the corresponding interparticle photo-dimerization process of the cyclobutane ring with photo-functional groups occurs on the modified silica surface.

4-2. Experimental

4-2-1 Materials and surface modification

Fumed silica powder, Aerosil® OX50 (OX50), was obtained from Nippon Aerosil Co., LTD.

Cinnamyl alcohol and cinnamoyl chloride with photo-functional groups were used as the modifier, and the physical properties of the two photo-functional groups are shown in Table 4-1.

Table 4-1. Physical properties of cinnamyl alcohol and cinnamoyl chloride.

Modifier	Cinnamyl alcohol	Cinnamoyl chloride
Formula	C ₉ H ₁₀ O (C ₆ H ₅ CH=CHCH ₂ OH)	C ₉ H ₇ ClO (C ₆ H ₅ CH=CHCOCl)
Molecular weight	134.18	166.6
Melting point	33 °C	35-36 °C
Boiling point	250 °C	256-258 °C
Manufacture	KANTO CHEMICAL CO.,INC	KANTO CHEMICAL CO.,INC

As both photo-functional groups can initiate a reaction when exposed to natural light, these experiments were carefully carried out in the dark. For the surface modification with cinnamyl alcohol, the autoclave method was performed at 270 °C, and 30 atm for 1 h with hexane used as the solvent [31, 32]. An additional amount of modifier was then changed from 0.25 to 20 number of modifiers per nm² on the modified silica surface related to the specific surface area of 2g of OX50. After the reaction, the sample was dried in a nitrogen atmosphere at above 70 °C. For the modification with cinnamoyl chloride, the reaction was carried out by the reflux method [33]. OX50 (2.0 g) was dispersed in 62.5mL of hexane and a certain amount of cinnamoyl chloride was then dissolved. The additional amount of cinnamoyl chloride was changed the same as for the modification using cinnamyl alcohol. The suspension was heated to reflux for 1 h at 68 °C, then the modified OX50 was washed with 80 mL of hexane 3 times and separated by pressure filtration, followed by drying under reduced pressure. Surface modification was carried out by the reactions of the cinnamyl alcohol and cinnamoyl chloride molecules with the hydroxyl groups on the silica surface according to the following equations:



4-2-2 Characteristics of silica surface

Qualitative analysis of the modifier on the surface of the modified OX50 was evaluated by FT-IR (Jasco FT/IR-620 spectrometer, Jasco Corporation), and the purpose of this characterization was to determine the decrease in the hydroxyl groups and presence of the Si-O-C spectral peak. It is regarded that the spectral peak of Si-O-C was attributed to chemisorption of the modifier on the silica surface, thus the processing of the modified reaction can be confirmed by observing this peak. The FT-IR measurement was done at a resolution of 4 cm⁻¹ between 400 and 4000 and the scan number was 200. The sample was molded into a pellet and it was then placed in a vacuum measuring cell [34].

The surface modifier density was estimated from the amount of modifiers and the specific surface area. Quantitative analysis of the modifier groups was obtained from the TG/DTA performed using a Rigaku Thermo plus TG8120 (Rigaku Corporation) from 30 °C to 550 °C at the heating rate of 20 °C/min in flowing air at 250 mL/min.

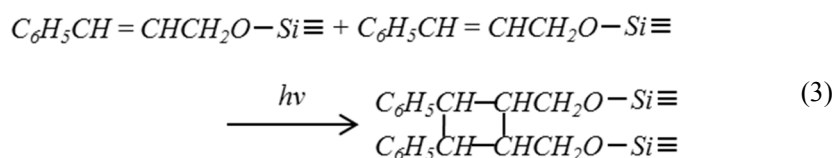
4-2-3 Determination of hydrophilic/hydrophobic

In order to determine the hydrophobic or hydrophilic properties of the modified silica surface,

the sample powders were dropped into the water, while the floating nature was judged by visual observation. The hydrophilic powders sank in the water, while the hydrophobic ones floated [35, 36].

4-2-4 Simulation

The modified silica forms a dimer structure through the cyclobutane-ring with C=C bonds by optical irradiation due to the photo-irradiation reaction described as follows:



The, simulation results provided information about the UV absorbing spectrum of the α and β -dimer structure of the modifiers by optical irradiation.

This simulation was carried out using the software “CACHe4.4” produced by Fujitsu Limited, and the MP3 method of MOPAC was selected for the structural optimization. In addition, the UV absorption spectrum was calculated by ZINDO which is a semi-empirical quantum chemistry method.

4-2-5 Optical irradiation and UV spectral characteristics of modified silica surface

1. Determination of tablet molding condition

The optimum condition for the tablet molding of the modified silica used in the photo-irradiation

experiment was determined by nitrogen adsorption, which could determine the pore sizes within the tablet samples [37].

The nitrogen adsorption measurements were performed using a Gemini manufactured by the Shimadzu Co., Japan. The measurement range of P/P_0 was between 0.7 and 0.99 with plot numbers of 30. The tablet samples of the silica powder were molded under various pressures, (20, 50 kgf/cm²) and not molded.

2. Optical reaction of modified silica

Due to the photo-dimerization of the modifiers, a photoreaction was observed by a UV spectrometer using on UV3100PC manufactured by the Shimadzu Corporation during the photo irradiation experiment. An extra high pressure mercury lamp (USHIO) covered with pyrex glass because of lightproof below 300 nm was selected as the optical source. The following are the other optical irradiation conditions: distance between the sample and optical source was 80 cm, the wattage was 350 W and the wavelength band emission was 300 nm to 500 nm. Acetonitrile and hexane were used as the solvents of the modifiers. On the other hand, when characterizing the surface modified silica, samples were formed into tablets which was confirmed to form the α bridge between the particles and measured by the diffuse reflex method.

4-3. Results and discussion

4-3-1 Characteristics of fumed silica

The corresponding transmission electron microscope (TEM) image of Aerosil® OX50 is shown in Fig. 4-1. As the sample is nonporous with a smooth surface, it is used to investigate the modified surface structures. The specific surface area of OX50 is 46.9 nm^2 measured by the BET method and the density of the surface hydroxyl groups for the unmodified sample was determined to be $3.2 - \text{OH}/\text{nm}^2$ by the Grignard reagent method [38, 39].

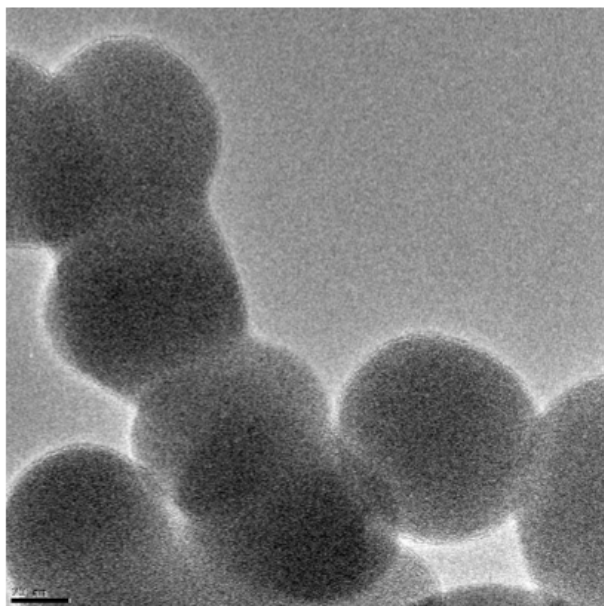


Fig. 4-1 TEM image of Aerosil® OX50.

4-3-2 IR spectral characteristics of silica surface

The FT-IR spectral characteristics of the silica with earlier reported data are shown in Table 4-2.

The FT-IR spectra of the unmodified OX50 and silica particles modified with various concentrations

of cinnamyl alcohol are shown in Fig. 4-2 and Fig. 4-3, respectively. Based on the curves, the silica bond absorption at 1868 cm^{-1} was determined based on the baseline of 2450 cm^{-1} in each sample. From Fig. 4-3, we can see that the -CH peak derived from the benzene ring located at 3066 cm^{-1} gradually increased with the increasing concentration of the cinnamyl alcohol, while the O-H stretching and adsorbed water decreased. In addition, the small peak that appeared at 963 cm^{-1} was assigned to the Si-O-C bond as shown in Fig. 4-4, which is attributed to the chemisorption modifier on the silica surface. It can be concluded that the surface modification was successfully performed by the chemical reaction of the cinnamyl alcohol molecules with the surface silanol groups by the autoclave method.

Table 4-2. FT-IR spectral characteristics of silica.

Frequency (cm ⁻¹)	Position assignment	Values reported earlier	References
963	Si-O-R	950-115	[40]
1623	Asymmetric Si-O-Si stretching	1102	[41, 42]
1868		1130-900	
1980			
1000-1300			
3066	Aromatic C-H stretching	3080 3110	[43]
3748	O-H stretching of Si-OH	3690	[42]

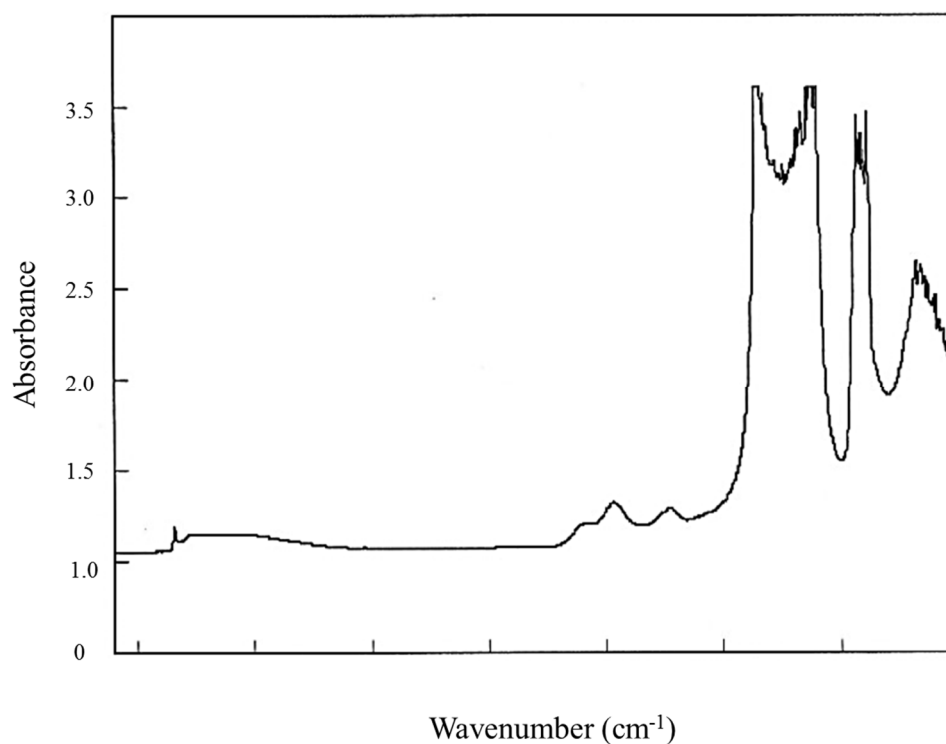


Fig. 4-2 FT-IR spectrum of the unmodified silica.

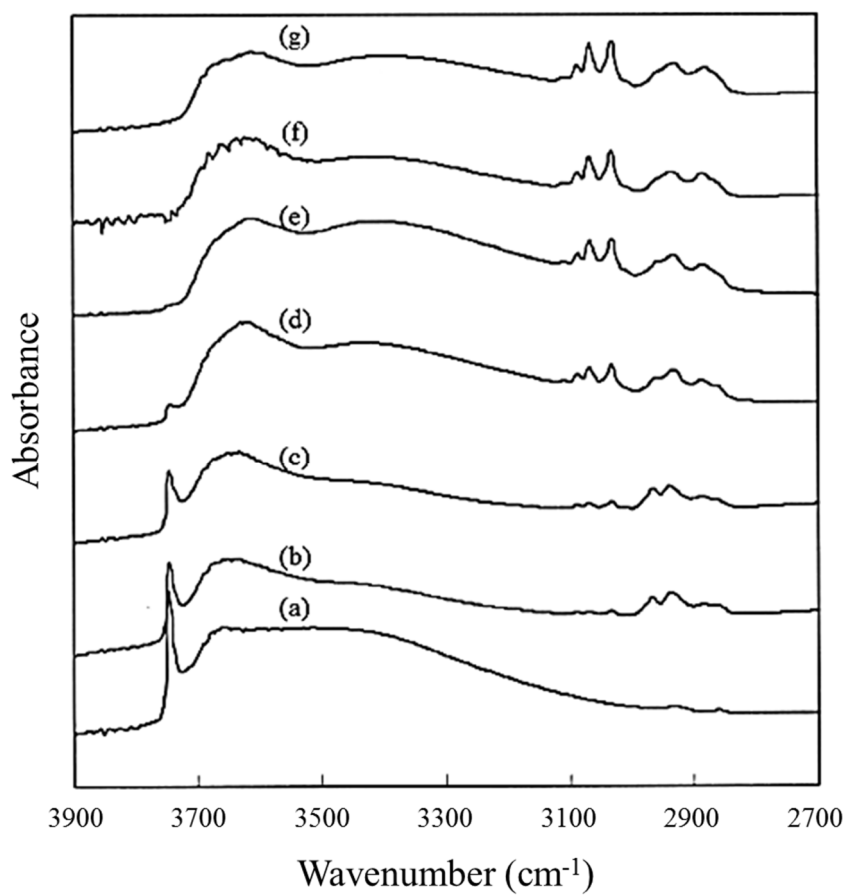


Fig. 4-3 FT-IR spectra of the unmodified and modified silica samples: (a) unmodified cinnamyl alcohol content was (b) 0.12 g/l (c) 0.23 g/l (d) 0.44 g/l (e) 1.60 g/l (f) 2.25 g/l (g) 4.46 g/l.

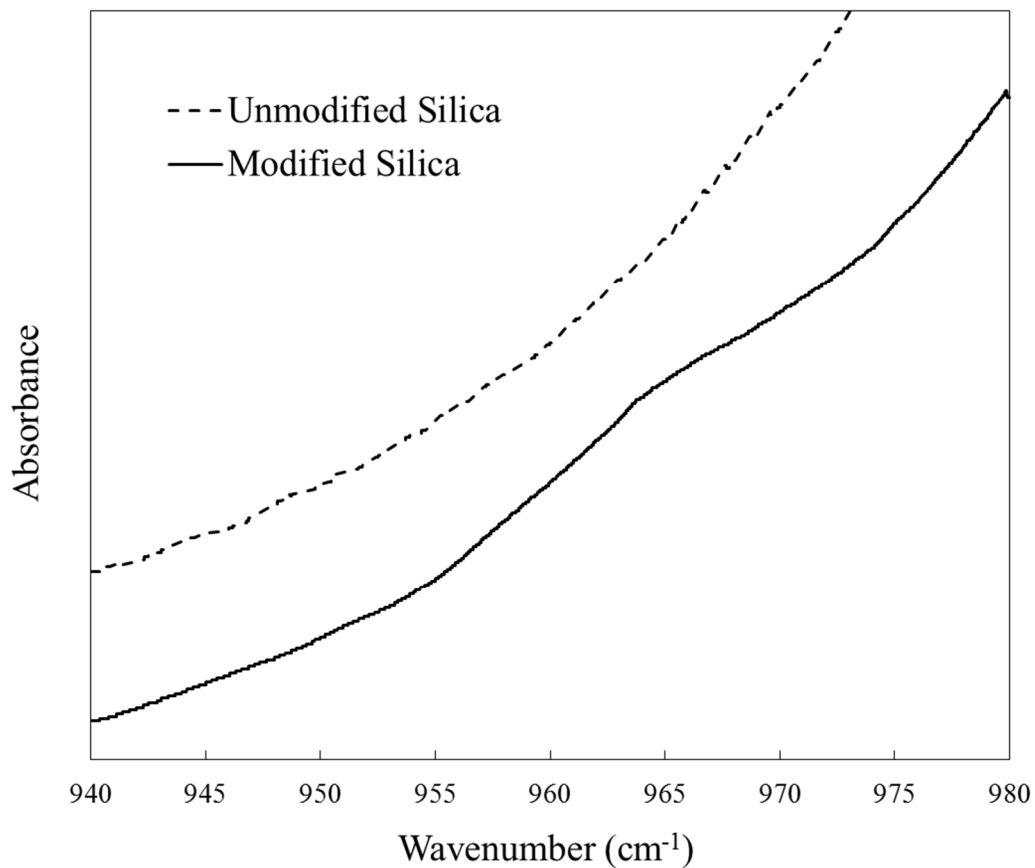


Fig. 4-4 FT-IR spectrum of Si-O-C at 963 cm⁻¹.

4-3-3 Determination of modifier introduced on silica surface

The number of modifier groups introduced onto the silica surface (dB) was calculated using equation (4), applying the weight losses of the modified sample (W_{CH}) and unmodified sample (W_{OH}).

$$dB(-OR/nm^2) = \frac{(\Delta w_{CH} - \Delta w_{OH})N_A}{M_w S_{N2}} \times 10^{18} \quad (4)$$

where ΔW_{CH} and ΔW_{OH} are the ratio of the weight loss for the modified and unmodified samples, respectively, measured by TG, MW is the molar weight of the modifier groups, S_{N_2} is the BET specific surface area measured from the nitrogen adsorption isotherm, and N_A is Avogadro's number [35].

The TG/DTA curves of the unmodified and modified silica were obtained by continuous heating at a definite temperature rate and the results are shown in Fig. 4-5 and Fig. 4-6, respectively. Based on the DTA curve, an exothermic reaction began around 270 °C, indicating that the burning of the modifier on the silica surface began at this temperature. Therefore, the amount of modifiers can be estimated from the weight loss in the TG curve in the combustion region of 270–550 °C, which in turn was determined by the DTA curve. In the case of the cinnamyl alcohol modified silica, the maximum surface density of the functional groups is 1.7 –OR/nm², and the relationship between the cinnamyl alcohol amount for the sample weight and surface density of the modification group is shown in Fig. 4-7. Meanwhile, two samples, which were modified with 0.44 and 3.23 mL/g cinnamyl alcohol, were used for the optical irradiation examination.

On the other hand, the maximum surface density of the modifier group was about 0.33 –OR/nm² for the samples modified with cinnamoyl chloride by the reflux method, while the value can be increased to 0.69 –OR/nm² with pyridine as the catalyst.

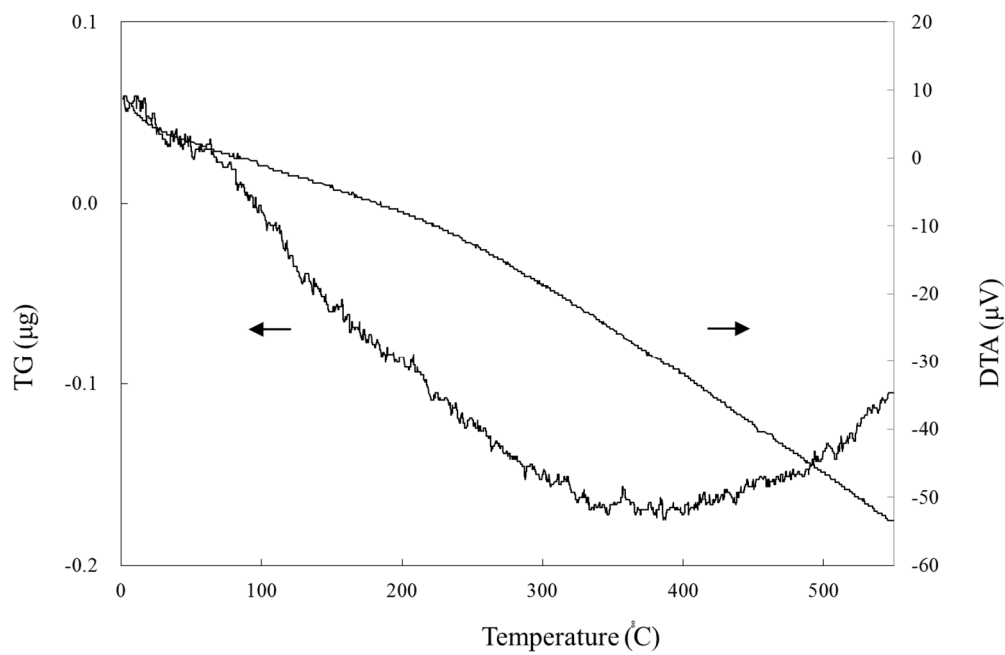


Fig. 4-5 TG/DTA curve for unmodified silica.

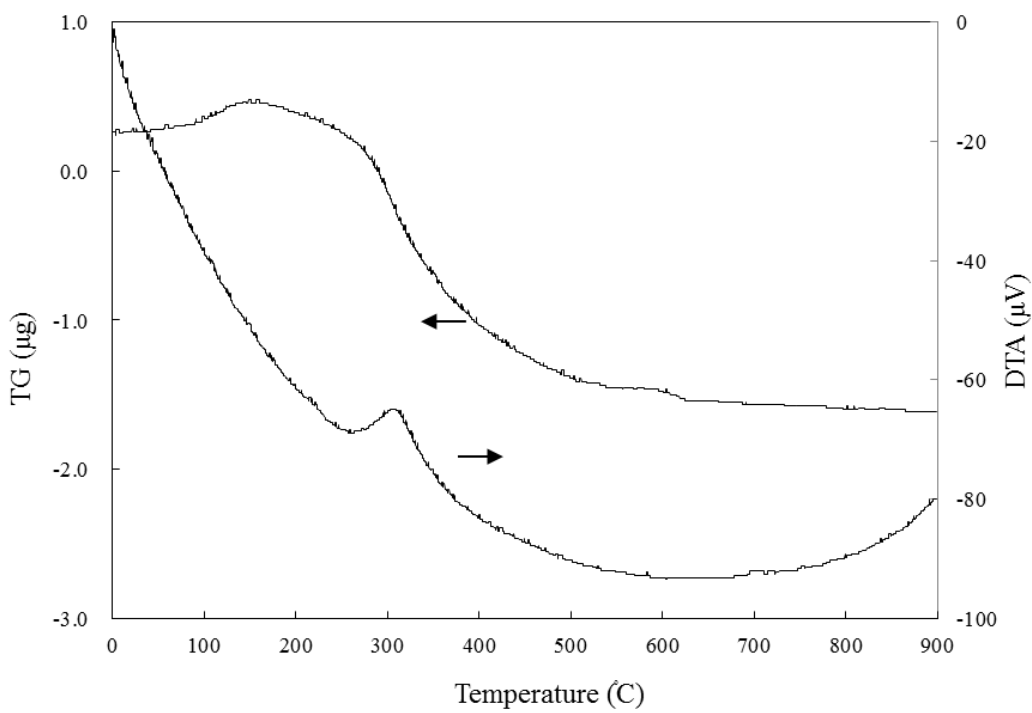


Fig. 4-6 TG/DTA curve for modified silica.

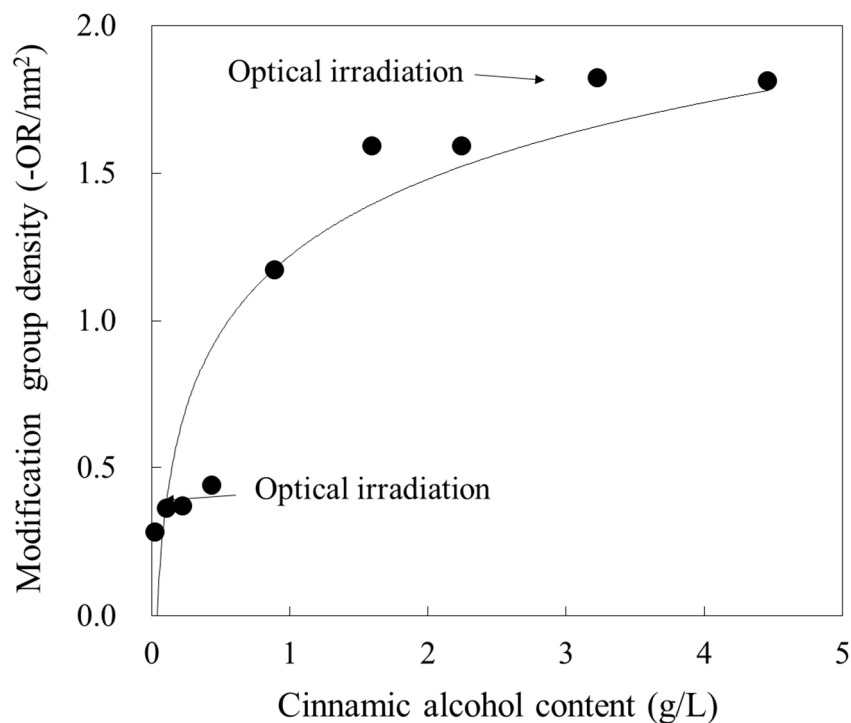


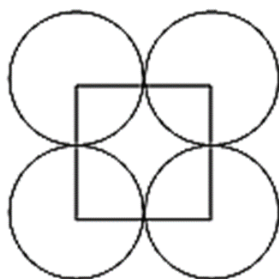
Fig. 4-7 Relationship between cinnamyl alcohols contents for sample weight and surface density of modification groups.

4-3-4 Determination of hydrophilic/hydrophobic

The unmodified silica sank in the water due to its hydrophilicity, while the modified sample floated on the water because of its hydrophobicity. The hydrophobic propensity was observed in a sample with the modifier density of 1.0 $-OR/nm^2$ and a higher density still results in surface hydrophobicity. Based on these results, it is postulated that the surface of the silica was uniformly-modified by the cinnamoyl groups at a modifier density greater than 1.0 $-OR/nm^2$ [44].

4-3-5 Calculation of the intermolecular distance

The intermolecular distance was calculated assuming that the modifiers were present in the most densely packed state on the silica surface. Their formulas and image diagrams are shown in Fig. 4-8. The intermolecular modifier distance for the sample with the surface density of 1.8 -OR/nm^2 was calculated to be about 0.75 nm, while the value for the sample with 0.4 -OR/nm^2 was about 16 nm. According to the established topo chemistry concept by Schmidt et al., the reactive double bonds are located parallel and the minimum distance between each other is 0.36–0.42 nm in the photo-dimerized olefin crystal [45]. Taking this concept into account, the dimers could not be formed in the calculated intermolecular distance. However, this calculation result was just an average distance determined from the surface modification density. It is considered that the surface modifiers are not evenly distributed and some modifiers might actually exist closely-situated on the silica surface, which could possibly initiate the photo-dimerization.



Intermolecular distance (L) = 0.74 nm

$$1 : L2 = 1 : 1.8$$

Fig. 4-8 Formulas and image diagram of intermolecular distance of modifiers (The sample whose amounts of surface modifier groups is 1.8 -OR/nm^2).

4-3-6 Simulation

The structures of the monomer and α , β -photodimers for the cinnamyl alcohol are shown in Fig. 4-9, and it is considered that the α -dimer possibly formed interparticles whereas the β -dimer formed intraparticles. The UV absorption spectra for each structure of the cinnamyl alcohol and cinnamoyl chloride are shown in Fig. 4-10 and Fig. 4-11 respectively. Based on the results of these simulations, the maximum absorption was observed around 250nm on both modifiers. However, as these strong absorptions were observed on each monomer, these absorptions were not observed after formation of their dimers. It is postulated that for the monomer structure, the π -electron delocalization occurs on the benzene through the double bond of the alkene on the monomer structure. On the other hand,

because the alkene double bond disappears due to the formation of the cyclobutane ring, the π -electron is partially delocalized in the benzene. Additionally, the difference in the α , β -dimers is mainly for the adsorption peaks located at 200 nm, that is, the absorption around 200 nm decreased if the α -dimer is formed, while it increased if the β -dimer is formed.

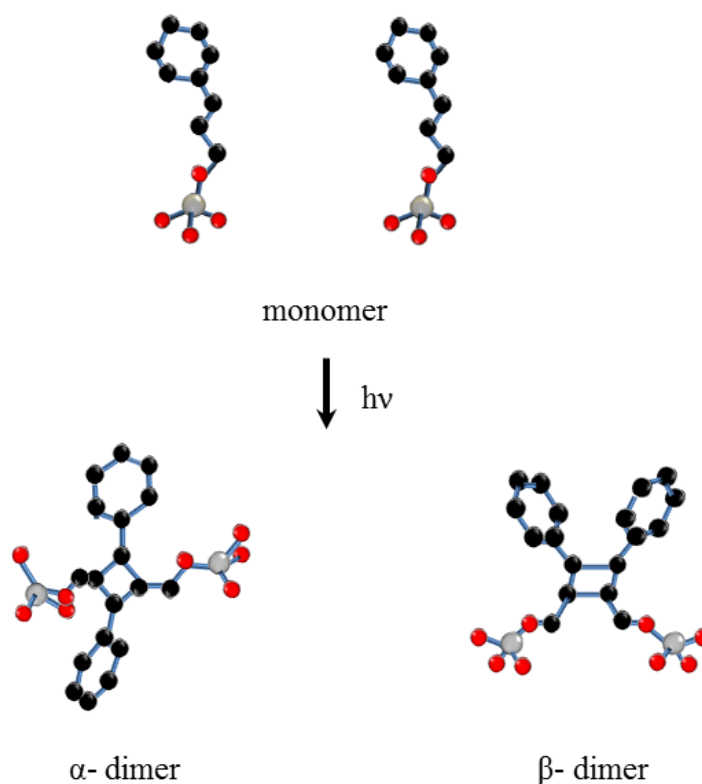


Fig. 4-9 Structure of monomer and α , β -dimers of cinnamyl alcohol by simulation.

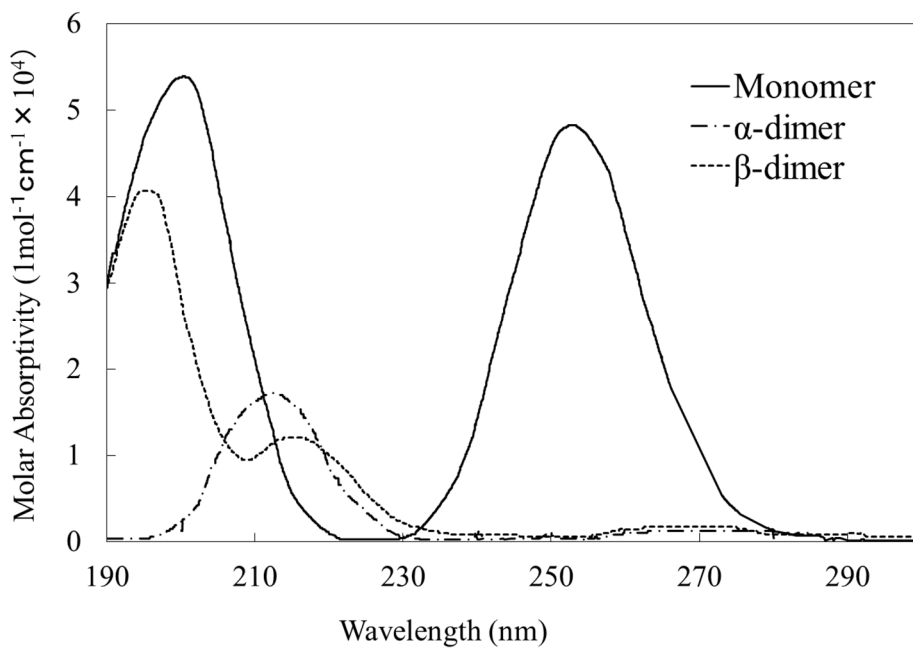


Fig. 4-10 UV adsorbing spectra of cinnamyl alcohol by simulation.

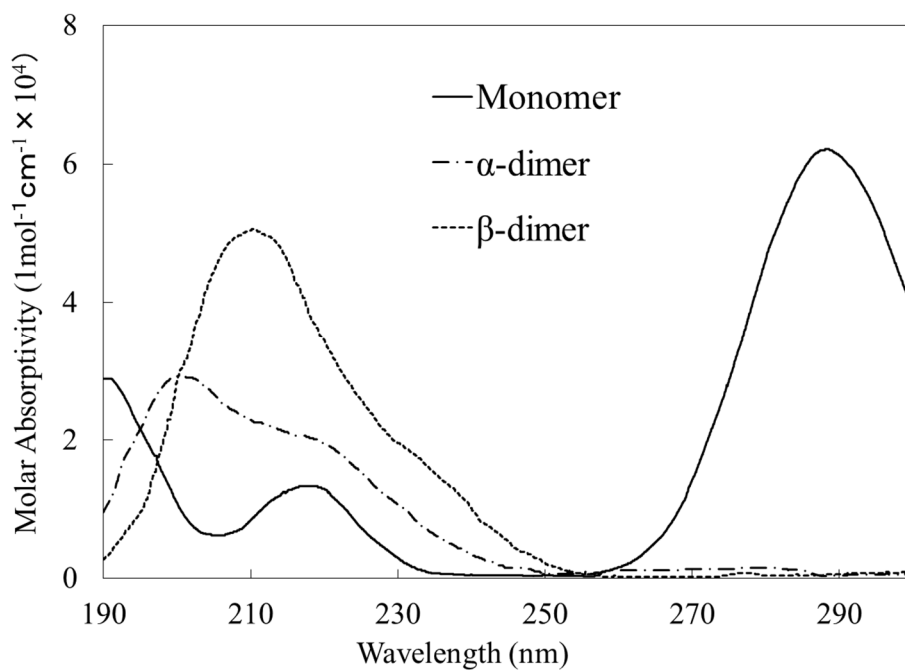


Fig. 4-11 UV adsorbing spectra of cinnamoyl chloride by simulation.

4-3-7 Optical irradiation

Fig. 4-12 shows the changes in the UV-absorption spectrum of the modifier in the organic solvent during the optical irradiation. It was observed that the 250 nm absorption decreased, which is in accordance with the simulation, suggesting that the modifier on the silica surface formed a photo-dimer by optical irradiation.

The pore size results of the tableting samples were provided by nitrogen adsorption, thus we could estimate how densely the silica particles were packed within each tablet. It is known that the initial pressure of the capillary condensation changes depending on the pore size of the tablet when measuring the nitrogen adsorption, and there is a correlation between the relative pressure at the beginning of the capillary condensation and radius of the capillary evaporation (kelvin radius, r_k), which is obtained by Kelvin's equation (5).

$$r_k (\text{\AA}) = -\frac{(2\gamma V_m \cos \theta)}{\{RT \ln(P/P_0)\}} \quad (5)$$

where P is the actual vapor pressure, P_0 is the saturated vapor pressure, γ is the surface tension, V_m is the molar volume of the liquid, R is the universal gas constant, θ is the contact angle, and T is temperature. The thickness of nitrogen multilayer has been reported by many researchers [46, 47]. Herein, the experimentally resolved multilayer thickness was calculated by formula (6) which was reported by Makinshima et al. using the Cranston-Inkley method.

$$t = 2.633 + 11.87\chi - 46.68\chi^2 - 385.8\chi^3 + 970.8\chi^4 - 1024.8\chi^5 + 395.9\chi^6 \quad (6)$$

where t is the multilayer thickness and χ is the relative pressure (P/P_0). Based on these formulas, the pore size was calculated and the tableting condition was determined [48, 49]. Based on the adsorption isotherm for nitrogen shown in Fig. 4-13, the capillary condensation began at about 0.995 P/P_0 in the tableting sample shape molded at 50 kgf/cm².

An r_k of 207 Å and a t of 14.3 Å were calculated by the kelvin equation, while the r_p was 221.3 Å as determined from the sum of r_k and t . Hence, it was found that the pore radius in the 50 kgf/cm² tablet sample was about 22 nm and such a sample has a moderate-density for the optical irradiation experiment. Therefore, it was expected that the modifiers on the silica surface would be situated within a reasonable distance to form the α -bridge between each other by applying the 50 kgf/cm² pressure.

Also, the UV-absorption spectrum changes for the modified sample with the surface density of 0.4 –OR/nm² and 1.8 –OR/nm² are shown in Figs. 4-14 and 4-15, respectively. Hence, the optical reaction rate of 1.8 –OR/nm² was lower than the 0.4 –OR/nm² sample, although the UV absorption was stronger. Additionally, the unmodified silica is not a UV absorber. It is expected that the surface modifier of the modified silica could react under optical irradiation and the reaction rate was determined by the modification density amount on the silica surface.

Also, in the case of the simulation result, the decrease in the adsorption at 250 nm can be observed due to the disappearance of the C=C. Therefore, the optical-dimer was formed on both modified sample surfaces in this experiment. In addition, in the 1.8 –OR/nm² case, it is expected that a large

volume of β -dimers will be formed as analyzed from the increase in the adsorption at 200 nm. On the other hand, in the case of 0.4 -OR/nm^2 , the α -dimers would be more easily formed than the β -dimers judging from the intermolecular distance. For the reasons noted above, if the β -dimers were formed on the silica surface, the modifier needs to be densely situated because they form intraparticles with the intermolecular distance of 7 \AA . Moreover, the α -dimers are mainly formed between different particles with the intermolecular distance of about 16 \AA . For these reasons, it is suggested that the surface modifier with a concentration of 1.8 -OR/nm^2 was densely packed, and thus the β -dimers were easily formed. The surface modifier with a concentration of 0.4 -OR/nm^2 was situated with enough space in the interparticles, leading to the tendency to form α -dimers. Based on these results, it was found that the modification with optical functional groups on the silica surface was achieved which led to the interparticle cross-linking.

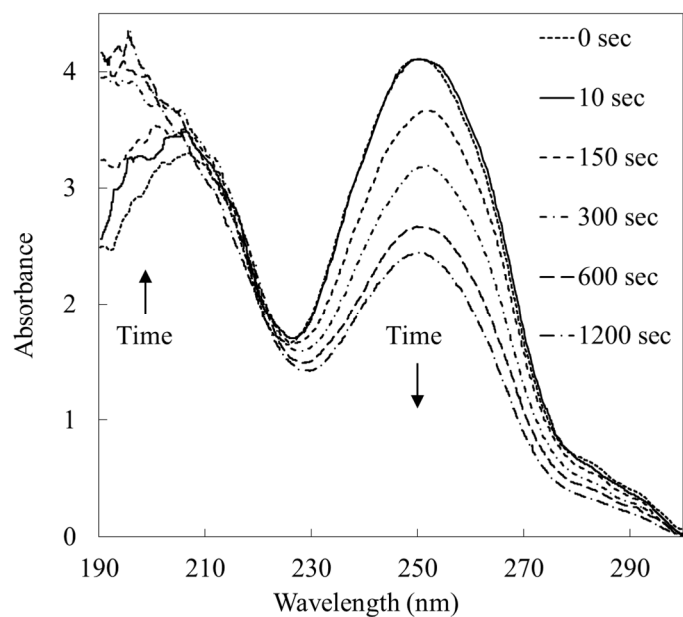


Fig. 4-12 UV absorbing spectrum change of modifier in organic solvent.

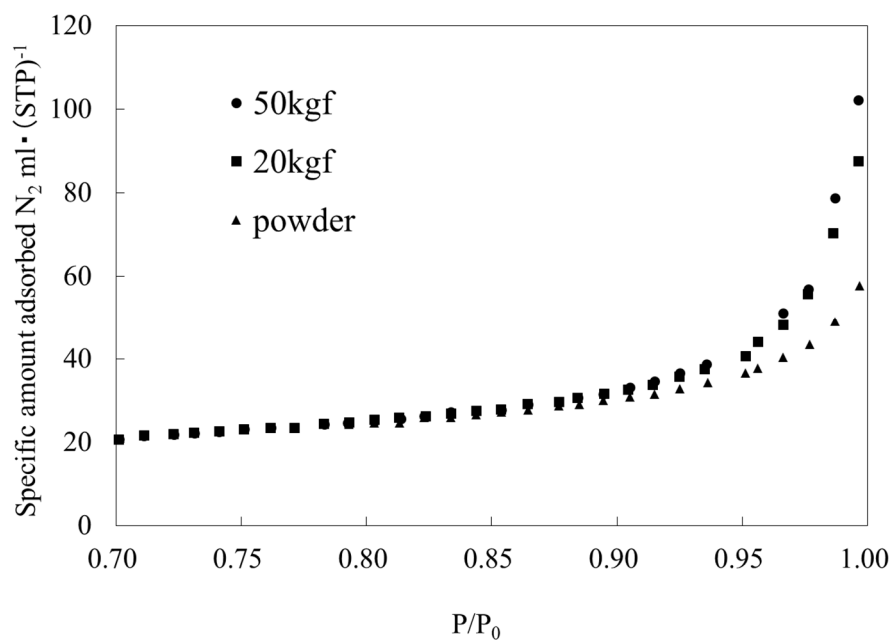


Fig. 4-13 Adsorption isotherm by nitrogen adsorption.

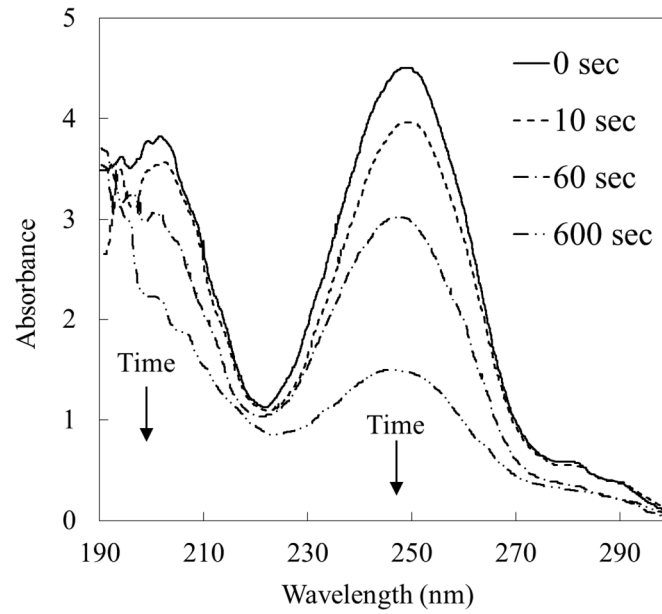


Fig. 4-14 UV absorbing spectrum change of modified sample of 0.4 -OR/nm^2 modification density.

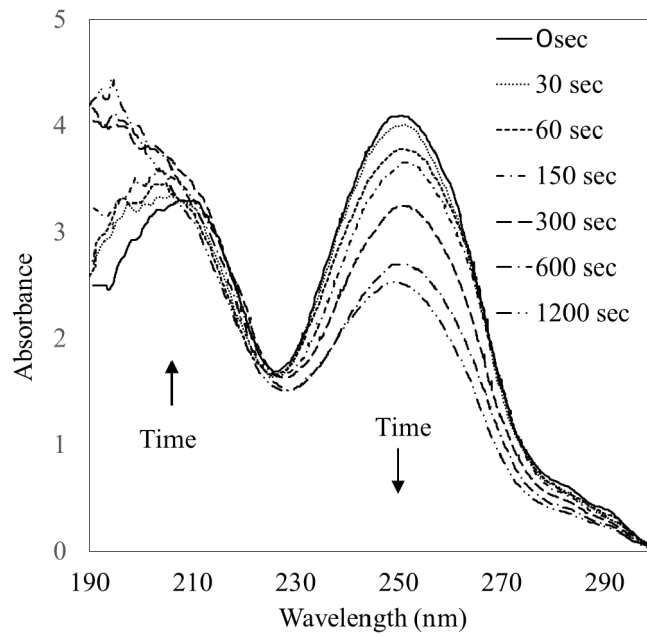


Fig. 4-15 UV absorbing spectrum change of modified sample of 1.8 -OR/nm^2 modification density.

4-4. Conclusion

In the present study, it was found that the surface modification density could be controlled by changing the initial concentration of the cinnamyl alcohol by the autoclave method, and the maximum modification density was 1.8 -OR/nm^2 . For the modification with cinnamoyl chloride, the density highly depended on the presence of a catalyst. In this case, the maximum modification density was only 0.33 -OR/nm^2 , but can be increased to 0.69 -OR/nm^2 with pyridine as the catalyst. Moreover, α and β -dimers were formed by photo reaction of the surface cinnamoyl groups on these modified silicas. The structure of the dimers on the modified silica surface was mainly affected by the surface modification density, which can be interpreted as the intermolecular distance. If the surface modification density is high, the surface cinnamoyl groups are close to each other, and they could form β -dimers. In contrast, if the surface modification density is low, sufficient space between the surface cinnamoyl groups could be created and could be more favorable for forming the α -dimers. It was suggested that the formation of α -dimers was necessary to form the three dimensional structures. However, the surface modifiers on the silica surface should not be densely packed for forming the α bridge within the interparticles.

References

- [1] S. Bose, S. V, Amit B, Bone tissue engineering using 3D printing, *Mater. Today*, 16 (2013) 496-504.
- [2] L. S. Dimas, G. H. Bratzel, I. Eylon, M. J., Buehler, Tough Composites Inspired by Mineralized Natural Materials: Computation, 3D printing, and Testing, Dimas, *Adv. Funct. Mater.*, 23 (2013) 4629–4623.
- [3] T. Yoshimura, M. Yoshimura, Design and creation of a molecular model for a 3D printer, *J. Technol. Educ.*, 21 (2014) 9–16.
- [4] B. Berman, 3-D printing: The new industrial revolution, *Business Horizons* 55 (2012) 155–162.
- [5] D. T. Pham, R. S. Gault, A comparison of rapid prototyping technologies, *Int. J. Mach. Tools Manuf*, 38 (1998) 1257–1287.
- [6] F. Doreau, C. Chaput, T. Chartier, Stereolithography for manufacturing ceramic parts, *Adv. Eng. Mater.*, 2 (2000) 493–496.
- [7] T. Chartier, C. Chaput, F. Doreau, M. Loiseau, Stereolithography of structural complex ceramic parts, *J. Mater. Sci.*, 37 (2002) 3141–3147.
- [8] C. W. Hull, (Uvp, Inc.) US4475330A 1986.
- [9] C. W. Hull, (3D Systems, Inc.) US4929402A 1990.
- [10] C. W. Hull, (Uvp, Inc.) US5569431A 1996.

- [11] I. Zeina, D. W. Hutmacherb, K. C. Tanc, S. H. Teoha, Fused deposition modeling of novel scaffold architectures for tissue engineering applications, *Biomaterials*, 23 (2002) 1169–1185.
- [12] D. W. Hutmacher, T. Schantz, I. Zein, K. W. Ng, S. H. Teoh, K. C. Tan, Mechanical properties and cell cultural response of polycaprolactone scaffolds designed and fabricated, *J. Biomed. Mater. Res. Part A*, 55 (2011) 203–216.
- [13] S. H. Ahn, M. Michael, D. Odell, S. Roundy, P. K. Wright, Anisotropic material properties of fused deposition modeling ABS, *Rapid Prototyping Journal*, 8 (2002) 248–257.
- [14] Mott, M. and Evans, J. R. G., Zirconia/alumina functionally graded material made by ceramic ink jet printing, *Mater. Sci. Eng.*, 1999, A271, 344–352.
- [15] E. Oezkol, J. Ebert, A. M. Waetjen, K. Uibel, R. Telle, Development of high solid content aqueous 3Y-TZP suspensions for direct inkjet printing using a thermal inkjet printer, *J. Eur. Ceram. Soc.*, 29 (2009) 403–409.
- [16] X. Zhao, J. R. G. Evans, M. J. Edirisinghe, Song, J. H., Direct ink-jet printing of vertical walls, *J. Am. Ceram. Soc.*, 85 (2002) 2113–2115.
- [17] R. Noguera, M. Lejeune, T. Chartier, 3D fine scale ceramic components formed by ink-jet prototyping process, *J. Eur. Ceram. Soc.*, 25 (2005) 2055–2059.
- [18] J. Guenster, A. Gahler, J. G. Heinrich, Rapid prototyping of ceramic components. *Ceramic Forum International*, 83 (2006) 53–56.

- [19] J. M. Williamsa, A. Adewunmib, R. M. Scheka,c, C. L. Flanagan, P. H. Krebsbacha,c, S. E. Feinbergd, S. J. Hollistera,b,e, S. Das, Bone tissue engineering using polycaprolactone scaffolds fabricated via selective laser sintering, *Biomaterials* 26 (2005) 4817–4827.
- [20] D. L. Bourell, H. L. Marcus, J.W. Barlow, J. J. Beaman, Selective laser sintering of metals and ceramics, *Int. J. Powder Metall.*, 28 (1992) 369–381.
- [21] H. Exner, L. Hartwig, H. Streek, M. Horn, S. Kloetzer, R. Ebert, R. et al., Laser micro sintering of ceramic materials. *Ceramic Forum International*, 63 (2006) 44–52.
- [22] R. Lenk, A. Naagy, H. J. Richter, A. Techel, Material development for laser sintering of silicon carbide. *Ceramic Forum International*, 83 (2006) 41–43.
- [23] A. M. Waetjen, D. A. Polsakiewicz, I. Kuhl, R. Telle, H. Fischer, Slurry deposition by airbrush for selective laser sintering of ceramic components, *J. Eur. Ceram. Soc.*, 29 (2009) 1–6.
- [24] P. Calvert, Inkjet Printing for Materials and Devices, *Chem. Mater.*, 13 (2001) 3299–3305.
- [25] F. Bauer, R. Flyunt, K. Czihal, H. Langguth b, R. Mehnert, R. Schubert, M. R. Buchmeiser, UV curing and matting of acrylate coatings reinforced by nano-silica and micro-corundum particles, *Prog. Org. Coat.*, 60 (2007) 121–126.
- [26] G. Chen, S. Zhou, G. Gu, H. Yan, L. Wua, Effects of surface properties of colloidal silica particles on redispersibility and properties of acrylic-based polyurethane/silica composites, *J. Colloid Interface Sci.*, 281 (2005) 339–350.

- [27] Y. Abe, Current Status and Updates on Radiation Curing Resin for Coating Technology, DIC Technical Review, 11 (2005).
- [28] K. Saigo, [2+2] Photocyclization and Photoreversion in Polymer Chemistry, J. Synth. Org. Chem Jpn., 73 (2015) 1006–1016.
- [29] T. Yamaoka, Photosensitive Polymer Materials, Polymers, 35 (1986) 572–575.
- [30] K. Akamatsu, T. Koide, Y. Kishimoto, M. Takayama, Applied Technology of Photosensitive Resin, Trade ed., CMC Publishing Co., Ltd., 2009.
- [31] K. R. Lange, Reactive organic molecules on silica surfaces, Chem. Ind., 36 (1969) 1273–1274.
- [32] H. Utsugi, Surface modification of oxide powders and the properties of the modified surfaces, Hyomen, 11 (1973) 591–609.
- [33] H. Utsugi, T. Matsuzawa, A. Akashima, Dehydration and Surface-Treatment of Silica Gels with Alcohols in Hydrocarbons with High Boiling Point by Reflux Method, Zairyo, 24 (1975) 638–642.
- [34] M. Fuji, C. Takai, Y. Tarutani, T. Takei, M. Takahashi, Surface properties of nanosize hollow silica particles on the molecular level, Adv. Powder Technol., 18 (2007) 81–91.
- [35] M. Fuji, S. Ueno, T. Takei, T. Watanabe, M. Chikazawa, Surface structural analysis of fine silica powder modified with butyl alcohol, Colloid. Polym. Sci., 278 (2000) 30–36.
- [36] H. Utsugi, T. Matsuzawa, A. Akoshima, Surface Properties of Silica Gels Treated with Alcohols in Long Chain Hydrocarbons by Reflux Method, Zairyo, 24 (1975) 643–648.

- [37] K. Sing, The use of nitrogen adsorption for the characterisation of porous materials, *Colloids Surf., A*, 187–188 (2001) 3–9. [38] J.J. Fripiat, J. Uytterhoeven, Hydroxyl Content in Silica Gel “AEROSIL”, *J. Phys. Chem.* 66 (1962) 800.
- [39] T. Kanazawa, M. Chikazawa, T. Takei, K. Mukasa, *Surface Chemistry of Powder Particles and Adhesion Phenomenon*, *Yougyo Kyokai shi* 92 (1984) 654.
- [40] T. Oh, C. K. Choi, Comparison between SiOC Thin Films Fabricated by Using Plasma Enhance Chemical Vapor Deposition and SiO₂ Thin Films by Using Fourier Transform Infrared Spectroscopy, *Journal of the Korean Physical Society*, 56 (2010) 1150–1155.
- [41] S. K. Parida, S. Dash, S. Patel, B.K. Mishra, Adsorption of organic molecules on silica surface, *Adv. Colloid Interface Sci.*, 121 (2006) 77–110.
- [42] T. I. Chun, V. Rossbach, Polymerization of Tetraethoxysilane by Using Remote Argon/dinitrogen oxide Microwave Plasma, *Jurnal of the Korean Society of Dyers and Finishers*, 21 (2009) 19–25.
- [43] N. Solc, O. Dopfer, Protonated Benzene: IR Spectrum and Structure of C₆H₇⁺, *Angewandte Chemie International Edition*, 41 (2002) 3628–3631.
- [44] M. Fuji, T. Takei, T. Watanabe, M. Masatoshi, Wettability of fine silica powder surfaces modified with several normal alcohols, *Colloids Surf., A*, 154 (1999) 13–24.
- [45] M. Hasegawa, [2+2] Topochemical Photoreaction, *J. Synth. Org. Chem Jpn.*, 46 (1988) 767–

775.

[46] K. Kaneko, Adsorption of Gasses, J. Jpn. Society of Color Mater., 67(1994) No. 2 115–123.

[47] S. Kondo, T. Ishikawa, I. Abe, Chemistry of Adsorption, 2nd ed., Maruzen Co., Ltd., 2006.

[48] F. Ohashi, M. Maeda, M. Suzuki, S. Tomura, M. Okazaki, K. Toriyama, Water Vapor Adsorption Properties of Ti-Containing Mesoporous Silica, J. Ceram. Soc. Jpn., 107 (1999) No.9 844–849.

[49] A. Makishima, T. Sasaki, T. Sakaino, Pore Structure of Porous Materials and Adsorption Isotherms, J. Ceram. Assoc., Jpn., 77 (1969) 225–233.

Chapter 5: Summary

Dispersible and aggregatable fumed silica was synthesized with the aim of developing methods for controlling the dispersibility and aggregability of nanosized particles. This thesis is divided into the following five chapters:

Chapter 1 is an introduction to fumed silica and its surface characteristics as well as the methods used for modifying its surface.

Chapter 2 describes the results of the investigation of the relationship between solvent polarity and the amount of water adsorbed on the surfaces of fumed silica particles; this relationship has a significant effect on the surface modification of fumed silica. The modification conditions play a key role in the modification of fumed silica at the molecular level. The experimental results revealed that the solvent polarity, solubility of the modifier, and amount of water adsorbed on the silica surface affect the surface modification rate in the liquid phase. The modification rate was high when the non-polar solvent hexane was used. It was observed that the water molecules adsorbed on the silica surface form a “layer” owing to the difference in their polarity and that of the solvent and that the amount of water adsorbed affects the surface modification rate. Based on the results presented in Chapter 2, it can be concluded that the relationship between solvent polarity and the amount of water adsorbed is important for designing nanosized materials with the desired functionality. It is suggested that the

interaction between solvent polarity and the adsorbed water can be exploited to control the number density of the modifier at the molecular level.

Chapter 3 describes the investigation performed to elucidate the effects of the structure and mobility of the modifier introduced on the fumed silica surface. The surfaces of fumed silica nanoparticles were modified with either *n*- or *t*-butyl alcohol at various concentrations. The changes in the surface wettability were observed macroscopically based on water preference dispersion tests and microscopically through water vapor adsorption tests, which were performed using FT-IR. It was determined that the structure and mobility of the modifier determine the surface wettability of the modified fumed silica. Based on the results presented in this chapter, it can be concluded that the effects of the structure and mobility of the modifier on surface wettability can be observed at the molecular level based on the water vapor adsorption test performed using FT-IR. It is suggested that the wettability influences the dispersibility and aggregability of fumed silica. Therefore, wettability observations performed at the molecular level are essential for designing fumed silica nanoparticles with the desired functionality.

Chapter 4 describes the synthesis of dispersible and aggregatable fumed silica, which was designed based on the knowledge presented in Chapters 2 and 3. Two photo-dimerization substances, namely, cinnamyl alcohol and cinnamoyl chloride, were introduced on the surfaces of the fumed silica nanoparticles. The modified nanoparticles formed two types of dimer, α - and β -dimers, after a

photoinduced reaction of the surface cinnamoyl groups. The structures of the dimers on the surfaces of the modified silica nanoparticles were primarily determined by the number density of the surface modifier, which can be considered the intermolecular distance. When the number density is low, there is enough space between the surface cinnamoyl groups for α -dimers to form. It is suggested that the formation of α -dimers is necessary for the realization of three-dimensional structures. Based on the results described in Chapter 4, the dispersible and aggregatable fumed silica design and synthesis at molecular level, and it confirmed their function by UV irradiation.

Based on the above-mentioned results, it can be concluded that elucidating the relationship between solvent polarity and the surface-adsorbed water is essential for the surface modification of fumed silica at the molecular level. The modification rate is probably determined by the interaction between solvent polarity and the water adsorbed on the surfaces of the fumed silica particles. In addition, the structure and mobility of the modifier significantly affect the surface wettability of fumed silica. It was determined that the wettability can be used as a molecular-level indicator of the properties of the modified surfaces of fumed silica nanoparticles. Based on these factors, a method for synthesizing dispersible and aggregatable fumed silica was proposed. Further, dispersible and aggregatable fumed silica was successfully synthesized using the proposed method, confirming that the method, which is based on molecular-level information, is an effective one.

Achievements

1. Effect of solvent polarity and adsorbed water on reaction between hexyltriethoxysilane and fumed silica.
A. Kawamura, M. Fuji, C. Takai, T. Shirai, *Colloid Surface A.*, Vol.492, pp. 249–254, (2016).
2. Surface modification of fumed silica by photo-dimerization reaction of cinnamyl alcohol and cinnamoyl chloride.
A. Kawamura, M. Fuji, H. Liu, C. Takai, T. Takei, H. K. Razavi, *Adv. Powder Technol.*, Vol.27, pp. 765–772, (2016).
1. Effect of steric hindrance on surface wettability of fine silica powder modified by n- or t-butyl alcohol.
A. Kawamura, M. Fuji, S. Ueno, C. Takai, T. Takei, H. K. Razavi, *Adv. Powder Technol.*, *Accepted*.

Acknowledgement

I would like to thank Prof. Fuji Masayoshi who provided helpful comments and suggestions. Special thanks also go to Dr. Chika Takai and Dr. Hadi Razavi-Khosroshahi who gave me invaluable comments and warm encouragements. I would also like to express my gratitude to my family for their moral support and warm encouragements. Additionally, I would like to thank Advanced Low Carbon Technology Research and Development Program (ALCA) of the Japan Science and Technology Agency (JST). Moreover, this study was partially supported by the Adaptable and Seamless Technology Transfer Program through Target-driven R&D (A-STEP) of the Japan Science and Technology Agency (JST). I would also like to thank Nippon Aerosil Co., Ltd., for offering the material for this study. These all supportive cooperation that made it possible to complete this study.

Synthesis of dispersible and aggregatable nanoparticle by
controlling of modification on silica surface

June, 2017

A Doctoral Dissertation by

Aki Kawamura